



ELSEVIER

Physica A 250 (1998) 8–45

PHYSICA A

# Quantum phase transition in spin glasses with multi-spin interactions

Theo M. Nieuwenhuizen\* , Felix Ritort

*Van der Waals-Zeeman Laboratorium and Institute for Theoretical Physics, University of Amsterdam, Valckenierstraat 65, 1018 XE Amsterdam, The Netherlands*

Received 28 June 1997

---

## Abstract

We examine the phase diagram of the  $p$ -interaction spin glass model in a transverse field. We consider a spherical version of the model and compare with results obtained in the Ising case. The analysis of the spherical model, with and without quantization, reveals a phase diagram very similar to that obtained in the Ising case. In particular, using the static approximation, reentrance is observed at low temperatures in both the quantum spherical and Ising models. This is an artifact of the approximation and disappears when the imaginary time dependence of the order parameter is taken into account. The resulting phase diagram is checked by accurate numerical investigation of the phase boundaries. © 1998 Published by Elsevier Science B.V. All rights reserved.

*PACS:* 05.30.-d; 64.60.Cn; 64.60.Kw; 64.70.Pf; 75.10.Nr

*Keywords:* Quantum phase transitions; Spin glasses;  $p$ -spin models

---

## 1. Introduction

The interplay between thermal and quantum effects in condensed matter physics is a longly debated problem [1–4]. The main differences between both type of effects relies on their dissipative nature. Thermal physics is inherently dissipative and energy is not conserved, while quantum physics is governed by the Schrödinger equation where energy is conserved if the Hamiltonian does not depend on time. How to include relaxational effects in a systematic way in the regime where quantum effects are dominant is a very interesting open problem [5].

This question is of the most relevance concerning glassy systems (for instance structural glasses or spin glasses) which are manifestly non-equilibrium phenomena. Recent

---

\* Corresponding author.

developments in the understanding of the connections between real glasses and spin glasses [6,7] suggest that it is of interest to investigate that family of glassy models where the static-phase transition is continuous from a thermodynamic point of view (i.e. there is no latent heat) but the order parameter is discontinuous at the transition temperature. These models are characterized by a one-step replica symmetry-breaking (1RSB) solution at low temperatures [9–11] and the existence of a dynamic singularity reminiscent of a spinodal instability [12,13]. Let us summarize here the glassy scenario for this type of mean-field models. At a certain temperature (to be called  $T_A$ ) in the paramagnetic regime, the phase space splits up into different components or metastable states separated by high-energy barriers (divergent with the size of the system), hence they have infinite lifetime in the thermodynamic limit. The number of these components is exponentially large with the size of the system  $\mathcal{N}_s = \exp(S_c)$  where  $S_c$  is the configurational entropy or complexity. From a thermodynamic point of view, the appearance of a large number of states does not induce a thermodynamic phase transition at  $T_A$ . Only at a “Kauzmann” temperature  $T_K$  lower than  $T_A$ , a true thermodynamic phase transition (with replica symmetry breaking) is observed. At  $T_K$  the complexity  $S_c$  vanishes. Hence, the glass transition is driven by a collapse of the complexity (entropy crisis) [12–14]. This is the mean-field version of the Gibbs–DiMarzio scenario [15,16] for the glass transition. The dynamical behavior of the system in the region  $T_K < T < T_A$  is then dominated by the existence of a large number of components which trap the system for exponentially long time scales ( $\tau \sim e^{2N}$ , where  $N$  is the system size). Whether a sharp  $T_K$  exists in finite dimensions is still a largely unsolved problem (for recent numerical simulations see [17]).

In this direction, a thermodynamic picture of cooling experiments in spherical  $p$ -spin models [18] has been recently proposed. This new thermodynamic approach gives an explanation for the paradox of the Ehrenfest relations at the glass transition. The main new point in this approach is that the configurational entropy changes along the transition line [19].

If the glass transition is driven by a collapse of the configurational entropy, it is natural to ask how this scenario is modified in the presence of quantum fluctuations. Generally speaking, quantum-phase transitions appear when an external perturbation reaches a critical value at zero temperature. Because at zero temperature the entropy vanishes at any value of the external field, it is expected that the complexity should also vanish everywhere at zero temperature (at least if there is no ground-state degeneracy, and this is the situation for the mean-field models we will consider here). In the absence of complexity it is natural to suppose that any adiabatic process at zero temperature (for instance, a process in which the external field is slowly turned off) could take the system to the ground state of the system. If complexity were not fully removed at zero temperature such expectation would fail since at zero temperature, quantum tunneling processes could not take the system out of the traps during any adiabatic process, mainly because the height of the barriers is extremely large [62].

A hint to this problem was recently reported in Refs. [20,21] where it was shown that in a certain class of mean-field models where the Gibbs–DiMarzio scenario is valid,

like the random orthogonal model [8], the complexity vanishes at zero temperature. The transition turned out to be second order at zero temperature. That proof was obtained in the framework of the static approximation introduced by Bray and Moore [22]. How much general is this result beyond the static approximation and in other family of models (for instance, the quantum Potts model [23]) is still unclear.

A family of models which has received considerable attention during the past years are the spherical [24,25] and Ising [26,27]  $p$ -interactions spin-glass models. These models are also characterized by a classical continuous thermodynamic transition with a discontinuous jump in the order parameter. The purpose of this work is the study of the quantum-phase transition in this family of models in an external transverse field. The Ising case has been already considered in the literature and has revealed novel properties in the phase diagram. In particular, Goldschmidt [28] computed the phase diagram in the  $p \rightarrow \infty$  case, i.e. the random energy model of Derrida (hereafter referred as REM [29]) in a transverse field. In this case the static approximation is exact and computations can be easily carried out. Goldschmidt found a phase diagram with three different thermodynamic phases, two of them are paramagnetic and separated by a first-order thermodynamic phase transition with latent heat. The existence of first-order phase transitions in spin-glass models with a discontinuous transition has to be traced back to Mottishaw who studied the random energy model (REM) in an external anisotropy field [30]. Computations for finite  $p$  were done later on by Thirumalai and Dobrosavljevic [31]. They found that the thermodynamic first-order transition line ended in a critical point. Such a critical point is pushed up to infinite temperature in the  $p \rightarrow \infty$  limit. Thirumalai and Dobrosavljevic went further and computed corrections to the static approximation finding similar qualitative results at high temperatures. Such an investigation has been recently extended by De Cesare et al. [32] to the low  $T$  region. Corrections to the  $p \rightarrow \infty$  limit are generally complicated specially in the  $\beta \rightarrow \infty$  limit where the two limits have to be taken in the appropriate way. In a similar context, recent results by Franz and Parisi [33] also show the existence of a first-order line when two replicas are coupled in the  $T - \varepsilon$  plane where  $\varepsilon$  is the strength of the coupling between the replicas.

Some computations done in disordered quantum-phase transitions involve the static approximation (hereafter referred as SA) introduced by Bray and Moore [22]. This is a reasonable approximation close to the classical transition line (in particular, it predicts a decrease of the transition temperature as the external field is switched on), but turns out to be inaccurate at low temperatures where dynamical correlations in imaginary time start to play a role (this is the reason why the approximation is called static). To clarify better the physical meaning of the SA, we present an alternative derivation of the mean-field equations by introducing a solvable spherical version of the quantum-Ising model. We will show that the same scenario for the quantum transition is valid in both the quantum-spherical and quantum-Ising models in the SA as well as beyond it.

For pedagogical reasons we will analyze in detail first the spherical version of the classical model which is much simpler to solve. After that, we consider a quantum

version of the spherical spin system (recently introduced in Ref. [34]). We give all the details that occur in the definition and evaluation of the coherent state-path integral. After considering a few toy examples, we analyze the quantum-spherical  $p$ -spin model.

Next, we will consider the Ising case and estimate the corrections to the SA numerically solving the self-consistent mean-field equations. We will show that the approximation gives a reasonable estimate (within 10%) of the position of the line boundaries which progressively improves as  $p$  increases. Deficiencies of the SA for both models will be also identified at low enough temperatures, in particular, reentrance of the  $T - \Gamma$  boundary line is observed.

The paper is organized as follows. In Section 2 we introduce the  $p$ -spin spherical spin-glass model and a derivation of the thermodynamic behavior in a transverse field is obtained with classical and quantum spins. Section 3 presents the solution of the Ising case, the analysis in the SA and also beyond it. Section 4 presents the conclusions. Finally, some appendices are devoted to several technical points.

## 2. Spherical spins

In this section we will consider multi-spin interaction spherical models without and with quantization. The spherical model is defined by

$$\mathcal{H} = - \sum_{i_1 < i_2 < \dots < i_p} J_{i_1 i_2 \dots i_p} S_{i_1}^z S_{i_2}^z \dots S_{i_p}^z - \Gamma \sum_i S_i^x, \quad (1)$$

where  $\Gamma$  is the transverse field. The indices  $i_1, i_2, \dots, i_p$  run from 1 to  $N$  where  $N$  is the number of sites. The  $J_{i_1 i_2 \dots i_p}$  are couplings Gaussian distributed with zero mean and variance  $p!J^2/(2N^{p-1})$ . The spins have  $m$  components and are subject to the spherical condition

$$\sum_{i=1}^N \sum_{a=1}^m S_i^a{}^2 = Nm\sigma, \quad (2)$$

where  $\sigma$  is a given constant.

In what follows, we first consider the classical case.

### 2.1. Classical situation

The replica calculation for the classical spherical model without transverse field was described by Crisanti and Sommers (CS) [24,25]. The steps are straightforward: (1) consider  $Z^n$ ; (2) average it over disorder; (3) rewrite it in terms of

$q_{\alpha\beta} = (1/N) \sum_{i=1}^N S_{i\alpha}^z S_{i\beta}^z$ ; (4) insert factors

$$\begin{aligned} 1 &= \int_{-\infty}^{\infty} dq_{\alpha\beta} \delta \left( q_{\alpha\beta} - \frac{1}{N} \sum_{i=1}^N S_{i\alpha}^z S_{i\beta}^z \right) \\ &= \int_{-\infty}^{\infty} dq_{\alpha\beta} \int_{-\infty}^{\infty} \frac{Nd\hat{q}_{\alpha\beta}}{4\pi i} e^{1/2\hat{q}_{\alpha\beta} (Nq_{\alpha\beta} - \sum_i S_{i\alpha}^z S_{i\beta}^z)}. \end{aligned} \quad (3)$$

A similar representation of the spherical constraints introduces as Lagrange multipliers the “chemical potentials”  $\mu_x$ . After these steps, one interchanges the order of integrals. The remaining integrals over  $S_{i\alpha}^z$  are all Gaussian (this is the benefit of the spherical approximation) and can be integrated out. One is left with an integral over  $q_{\alpha\beta}$ ,  $\hat{q}_{\alpha\beta}$  and  $\mu$ , which can be taken at its saddle point. As for  $\Gamma = 0$ , the fields  $\hat{q}_{\alpha\beta}$  can be integrated out [24,25], and one ends up with the replicated free energy

$$\begin{aligned} 2\beta F_n &= -\frac{2}{N} \log(\bar{Z}_J^n) = -\frac{\beta^2 J^2}{2} \sum_{\alpha\beta} q_{\alpha\beta}^p - \text{tr} \ln q \\ &\quad + \sum_x \left\{ \beta \mu_x (q_{xx} - m\sigma) - \frac{\beta \Gamma^2}{\mu_x} + (m-1) \ln(\beta \mu_x) \right\}. \end{aligned} \quad (4)$$

As for the case  $\Gamma = 0$ , we assume a one-step replica symmetry-breaking pattern. This involves parameters  $u$ ,  $q_d$ ,  $q$ , and  $x$ . These are the chemical potential ( $\mu_x = \mu$ ), the replica self-overlap ( $q_{xx} = q_d$ ), the overlap between different replicas inside diagonal IRSB blocks ( $q_{\alpha\beta} = q$  for  $(\alpha, \beta)$  inside a block, while vanishing outside the  $x \times x$  blocks) and the breaking parameter in the Parisi scheme ( $x$  is size of block), respectively. Note that  $q_d$  are less than  $m\sigma$  since the spins can turn perpendicular to the  $z$ -axis. Following CS we obtain for  $n \rightarrow 0$  the “classical” free energy  $F_{cl} = F_n/n$ :

$$\begin{aligned} 2\beta F_{cl} &= -\frac{\beta^2 J^2}{2} (q_d^p - \xi q^p) - \frac{1}{x} \ln(q_d - \xi q) - 1 \\ &\quad + \frac{\xi}{x} \ln(q_d - q) + \beta \mu (q_d - m\sigma) - \frac{\beta \Gamma^2}{\mu} + (m-1) \ln(\beta \mu), \end{aligned} \quad (5)$$

where  $\xi = 1 - x$ . Optimization with respect to  $\mu$ ,  $q_d$ ,  $q$ , and  $x$  yields the saddle-point relations

$$q_d + \frac{\Gamma^2}{\mu^2} + \frac{(m-1)T}{\mu} = m\sigma, \quad (6)$$

$$\mu = \frac{p\beta J^2}{2} (q_d^{p-1} - q^{p-1}) + \frac{T}{q_d - q}, \quad (7)$$

$$\frac{p\beta^2}{2} q^{p-1} = \frac{q}{(q_d - q)(q_d - \xi q)}, \quad (8)$$

$$-\frac{\beta^2}{2} q^p + \frac{1}{x^2} \ln \frac{q_d - \xi q}{q_d - q} - \frac{q}{x(q_d - \xi q)} = 0. \quad (9)$$

The latter equation expresses that  $\partial F/\partial x = 0$ . This means that we consider thermodynamic equilibrium. For a discussion of the thermodynamics of slow cooling experiments, see Refs. [18,19].

## 2.2. The paramagnet and its pre-freezing line

Let us first consider the paramagnet, where  $q = 0$ . Like in the case of the  $p$ -spin Ising glass in a transverse field (see the next section), we find a first-order transition line separating two paramagnetic phases. This line is comparable with the boiling line of a liquid and has a critical endpoint. To find it we insert Eq. (7) with  $q = 0$  in Eq. (6) and obtain

$$\Gamma^2 = (m\sigma - q_d) \left( \frac{p\beta J^2}{2} q_d^{p-1} + \frac{T}{q_d} \right)^2 - (m-1) \left( \frac{pJ^2}{2} q_d^{p-1} + \frac{T^2}{q_d} \right). \quad (10)$$

At large  $T$  and  $\Gamma$  this has just one real positive solution  $0 < q_d < m\sigma$ . However, below a critical value  $T_{cep}$  there is a regime of  $\Gamma$ -values where there occur three solutions rather than one. The outer ones are stable, while the middle one is unstable. This critical endpoint (*cep*) has coordinates  $(T_{cep}, \Gamma_{cep})$ , determined by  $d\Gamma/dq_d = d^2\Gamma/dq_d^2 = 0$ . From this point, a first-order transition line originates towards the spin-glass phase and intersects it at the multi-critical point  $(T_{mcp}, \Gamma_{mcp})$  [35]. Along this line there is a finite latent heat that vanishes at the critical endpoint. It separates a small transverse field phase with large ordering in the  $z$ -direction ( $q_d^>$ ) from a phase with smaller ( $q_d^<$ ) ordering in the  $z$ -direction on the large field side.

In analogy with wetting phenomena, where a pre-wetting line occurs off coexistence, we call this *the pre-freezing line*. In order to motivate this term, let us first explain the situation of first-order wetting of a bulk fluid A by a thin layer of a fluid B [36,37]. At bulk coexistence of A and B phases there is a wetting temperature  $T_w$ . For  $T$  below  $T_w$  a finite layer (“wetting layer”) of B atoms will cover the A phase; for first-order wetting this layer remains finite in the limit  $T \rightarrow T_w^-$ . For  $T > T_w$  there will be an infinite B layer (“complete wetting”). When the fluids A and B are off coexistence there is a difference in chemical potential  $\Delta\mu$ . Let us take the convention that on the  $\Delta\mu < 0$ -side the B layer is always finite. Then when  $\Delta\mu \rightarrow 0^-$  for  $T < T_w$ , the B layer will reach its finite thickness discussed for  $\Delta\mu = 0$ . For  $\Delta\mu > 0^+$  it will be infinite however, leading to a discontinuous transition. For  $T > T_w$ , however, the thickness of the B-layer will diverge continuously in the limit  $\Delta\mu \rightarrow 0^-$ , in order to be infinite at  $\Delta\mu = 0$ , and it will remain infinite for  $\Delta\mu > 0$ . In that temperature regime there is a continuous transition at  $\Delta\mu = 0$ . Thermodynamics requires coexistence at a first-order transition line (called the “pre-wetting line”) which separates the regime of continuous and first-order wetting. The endpoint of this line is called the “pre-wetting critical point”. The pre-wetting line, occurrence of hysteresis, and, near the pre-wetting

critical point, scaling of the jump in coverage across the line have been observed in  $^4\text{He}$  on Ce [38] and for methanol–cyclohexane mixtures [39,40].

In our spin glass a similar situation occurs. The  $\text{SG-PM}^>$  line is a continuous transition line (in the sense that there is no latent heat), whereas we will find a finite latent heat at the  $\text{SG-PM}^<$  transition. Also, in this situation a first-order line with non-vanishing latent heat must emerge from the point  $(T_{mcp}, \Gamma_{mcp})$  and divide the paramagnet into two regimes. It is the line discussed, and by analogy we propose to call it the pre-freezing line. Its critical endpoint can then be called the “pre-freezing critical point”.

### 2.3. The spin-glass phase

This discontinuity of the paramagnet has no analog in the spin glass. There is only one spin-glass phase, namely the continuation of the  $q_d^>$  paramagnet, with continuous  $q_d$  at the transition line  $x = 1$ . We stress that this also holds when the  $\text{PM}^<$  phase is the thermodynamically stable phase: also then the (metastable) SG phase merges with the (metastable)  $\text{PM}^>$  phase at the  $x = 1$  line.

To check this continuity of the SG-phase, let us insert Eq. (8) into Eq. (9) and replace the  $x$ -dependence by dependence on a new variable  $\eta$  via

$$x = \frac{p-1-\eta}{\eta} \frac{q_d - q}{q}. \quad (11)$$

Eq. (9) then becomes

$$\ln \frac{p-1}{\eta} = \frac{(p-1-\eta)(\eta+1)}{p\eta} \quad (12)$$

which has a solution  $0 < \eta < 1$ . This shows that  $\eta$  is independent of  $\Gamma$  and  $T$ . (For  $\Gamma = 0$  this was noted already by Crisanti and Sommers [24,25].) Once  $\eta$  is known, we can choose  $x$  and solve  $q = (p-1-\eta)q_d / (p-1-\xi\eta)$  from Eq. (11). Eq. (8) will then yield

$$q_d = \frac{p-1-\xi\eta}{p-1-\eta} \left( \frac{2T^2(p-1-\eta)^2}{x^2\eta p(p-1)} \right)^{1/p}. \quad (13)$$

At fixed  $x$  we can vary  $T$ . We thus know  $q_d$  and  $q$ , and therefore find a curve  $\Gamma(T)$ . At small enough  $T$  two values of  $x$  can lead to a given point  $(T, \Gamma)$ ; we need the smallest of these two  $x$ -values. By varying  $x$  between 1 and 0 this procedure then uniquely determines the spin-glass phase.

The pre-freezing line intersects the  $\text{PM}^>$ -SG transition line at a multi-critical point  $(T_{mcp}, \Gamma_{mcp})$  [35].

Just as at  $\Gamma = 0$  the transition  $\text{PM}^>$ -SG occurs with  $x = 1$ . This is a thermodynamic continuous-phase transition. The SG free energy exceeds the  $\text{PM}^>$  one by an amount of order  $\xi^2$ . The transition  $\text{PM}^<$ -SG is thermodynamically first order and occurs with  $x < 1$ . The transition line is fixed by equating the free energies of the  $\text{PM}^<$  and the SG solutions.

## 2.4. Low-temperature behavior

The transition line between  $\text{PM}^<$  and SG will continue down to  $T = 0$ . Everywhere along this line there will be a latent heat accorded by a jump in entropy. For studying the low- $T$  behavior we set

$$q_d = (1 + Tr)q \quad (14)$$

which implies

$$x = \frac{p-1-\eta}{\eta} rT, \quad \frac{p(p-1)J^2}{2\eta} q^p r^2 = 1, \quad (15)$$

$$\mu = \frac{\eta}{qr} \frac{(1+rT)^{p-1} - 1}{(p-1)rT} + \frac{1}{qr}. \quad (16)$$

At  $T = 0$  this yields  $\mu = (\eta + 1)/qr$  and then

$$q + \frac{2\eta\Gamma^2}{p(p-1)(\eta+1)^2 J^2} q^{2-p} = m\sigma. \quad (17)$$

For  $p = 3$  it can be solved exactly

$$q = \frac{m\sigma}{2} + \sqrt{\frac{m^2\sigma^2}{4} - \frac{\eta\Gamma^2}{3(\eta+1)^2 J^2}}, \quad (18)$$

showing that the SG phase cannot exist at large  $\Gamma$ . For small  $\Gamma$  the spin-glass phase is stable; for larger values it becomes meta-stable and for still larger values it will be unstable. The free energy may be expanded in powers of  $T$ :

$$F = F_0 + T \left( -\frac{m}{2} \ln T + F_1 \right) + \mathcal{O}(T^2). \quad (19)$$

One finds

$$F_0 = -\frac{\eta+2}{2pr} - \frac{\Gamma^2 qr}{\eta+1},$$

$$F_1 = \frac{1}{2}(\eta+1 + (m-1)\ln(\eta+1) + m \ln qr). \quad (20)$$

In the paramagnet  $\text{PM}^<$  one has  $q_d \approx T\sqrt{m\sigma}/\Gamma$ ,  $\mu \approx \Gamma/\sqrt{m\sigma}$ , implying

$$F_0 = -\Gamma\sqrt{m\sigma}, \quad (21)$$

$$F_1 = \frac{1}{2} \left( 1 + m \ln \frac{\Gamma}{\sqrt{m\sigma}} \right). \quad (22)$$

Equating the  $T = 0$  results we find a transition at some  $\Gamma_c$ . For small  $T$  we get

$$F_{\text{SG}} - F_{\text{PM}} = A(\Gamma - \Gamma_c) + BT \quad (23)$$

with  $A > 0$  because the stable phase has lowest free energy, and

$$B = \frac{1}{2}(\eta - \ln(\eta+1)) + \frac{m}{4} \ln \frac{m\sigma}{m\sigma - q} \quad (24)$$

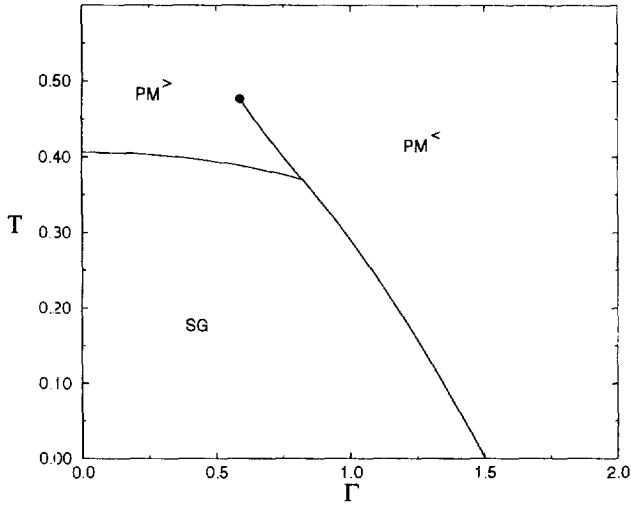


Fig. 1. Phase diagram for the classical spherical model for  $p = 4$ ,  $m\sigma = 1$ ,  $m = 2$ . The multi-critical point and the critical point are given by  $T_{mcp} = 0.3703$ ,  $\Gamma_{mcp} = 0.8208$ ,  $T_{cep} = 0.4767$ ,  $\Gamma_{cep} = 0.5878$  while at  $T = 0$ ,  $\Gamma_c = 1.503$ .

also positive. For small  $T$  the transition line has a linear slope

$$\Gamma = \Gamma_c - \frac{B}{A}T, \quad (25)$$

showing that there occurs no reentrance. For the case  $m = 2$  and in units where  $m\sigma = 1$ , the full-phase diagram for  $p = 4$  is shown in Fig. 1. In Fig. 2 we show the latent heat as a function of the temperature. It has been computed along the boundary lines starting from the critical point, following the  $PM^<$ - $PM^>$  and the  $PM^<$ - $SG$  lines. Note the existence of a sharp maximum at  $T = T_{mcp}$ .

### 2.5. Quantum spherical spins

Due to the form, Eq. (19), the entropy of spherical models diverges as  $(m/2)\ln T$  for small  $T$ . The related zero-temperature specific heat  $C = m/2$ , occurring due to the Gaussian nature of the spins, is analogous to the Dulong–Petit law of classical harmonic oscillators. In order to have a physical description in the low- $T$  regime, one of us recently proposed quantization by analogy with harmonic oscillators [34]. Here we present some details of this approach. It follows the standard Trotter–Suzuki approach of thermal field theories, see e.g. the book of Negele and Orland [41].

The approach starts from the Trotter formula of the path-integral representation of the partition sum, in which the coherent-state representation of the identity is restricted to coherent-states described by parameters which satisfy the spherical constraint. For a set of harmonic oscillators  $\mathbf{S} = \{S_i^a\}$  with  $(i = 1, \dots, N, a = 1, \dots, m)$  a coherent state

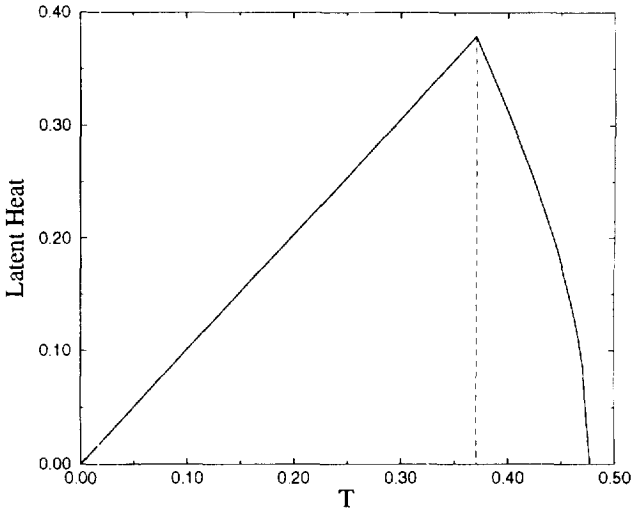


Fig. 2. Latent heat for the classical spherical model for  $p = 4$  versus  $T$  along the boundary line which separates the  $PM^<$  phase from the  $PM^>$  (right part above the multi-critical point) and SG phases (left part below the multi-critical point). There is a maximum at the multi-critical point (indicated by the dashed line).

is defined by

$$| \mathbf{S} \rangle = e^{\mathbf{S} \cdot \mathbf{S}_{op}^\dagger} | \mathbf{0} \rangle = \prod_{i,a} \left\{ \sum_{n_{ia}=0}^{\infty} \frac{(S_i^a)^{n_{ia}}}{\sqrt{n_{ia}!}} | n_{ia} \rangle \right\}, \tag{26}$$

where  $S_{i,op}^{a\dagger}$  is the creation operator of the harmonic oscillator ( $i, a$ ) and  $S_i^a$  is a  $c$ -number. The coherent states are overcomplete and have inner product

$$\langle \mathbf{S}' | \mathbf{S} \rangle = e^{\mathbf{S}' \cdot \mathbf{S}} \tag{27}$$

which can be checked in various ways. The coherent-state representation of the identity in Fock space reads in general

$$\begin{aligned} \mathbf{1} &= \prod_{i,a} \left\{ \sum_{n_{ia}=0}^{\infty} | n_{ia} \rangle \langle n_{ia} | \right\} \\ &= \int \prod_{ia} \frac{dS_i^{a*} dS_i^a}{\pi} e^{-\mathbf{S}^* \cdot \mathbf{S}} | \mathbf{S} \rangle \langle \mathbf{S} |. \end{aligned} \tag{28}$$

It was proposed by one of us [34] to enforce the spherical constraint by restricting this representation to coherent states which satisfy the spherical constraint

$$\mathbf{S}^* \cdot \mathbf{S} = \sum_{i=1}^N \sum_{a=1}^m S_i^{a*} S_i^a = Nm\sigma. \tag{29}$$

This is done by replacing

$$\mathbf{1} \rightarrow \mathbf{1}_{\text{spherical}} \equiv C \int \prod_{ia} \frac{dS_i^{a*} dS_i^a}{\pi} e^{-\mathbf{S}^* \cdot \mathbf{S}} |\mathbf{S}\rangle \langle \mathbf{S}| \delta(\mathbf{S}^* \cdot \mathbf{S} - Nm\sigma), \quad (30)$$

where the constant  $C$  will be fixed later. In a Trotter approach one calculates

$$Z = \text{tr} e^{-\beta H(\mathbf{S}_{op}^\dagger, \mathbf{S}_{op})} = \text{tr}(e^{-\varepsilon H(\mathbf{S}_{op}^\dagger, \mathbf{S}_{op})})^M \quad (31)$$

with  $\varepsilon = \beta/M$ . Between all factors  $\exp(-\varepsilon H)$  one inserts the coherent-state representation of the identity. For our spherical spins we have to choose the truncated versions, Eq. (30). Let us number them by  $j = 1, \dots, M$ . It was shown by Negele and Orland that for normal-ordered Hamiltonians

$$\langle \mathbf{S}_j | e^{-\varepsilon H(\mathbf{S}_{op}^\dagger, \mathbf{S}_{op})} | \mathbf{S}_{j-1} \rangle = e^{\mathbf{S}_j^* \cdot \mathbf{S}_{j-1} - \varepsilon H(\mathbf{S}_j^*, \mathbf{S}_{j-1})}. \quad (32)$$

The term  $\exp(\mathbf{S}_j^* \cdot \mathbf{S}_{j-1})$  arises from the overlap of the coherent states, Eq. (27), while the  $\varepsilon H$  correction can be found by expanding the exponential, using  $\mathbf{S}_{op} | \mathbf{S}_{j-1} \rangle = \mathbf{S}_{j-1} | \mathbf{S}_{j-1} \rangle$  and its Hermitean conjugate  $\langle \mathbf{S}_j | \mathbf{S}_{op}^\dagger = \langle \mathbf{S}_j | \mathbf{S}_j^*$ , and re-exponentiating the result. Corrections are of order  $\varepsilon^2$  and can be neglected in the limit  $M \rightarrow \infty$  (for a discussion, see Ref. [41]). Introducing the imaginary time variable  $\tau = j\varepsilon = j\beta/M$  and writing out the spherical constraints in terms of an imaginary-valued chemical potential  $\mu(\tau)$ , this leads to the coherent-state path integral representation or thermal field theory for spherical spins

$$Z = \int D\mu DS^* DS \exp(-A) \quad (33)$$

with integration measure

$$\int DS^* DS = \prod_{ia\tau} \int_{-\infty}^{\infty} \int_{-\infty}^{\infty} \frac{d\Im(S_i^a(\tau)) d\Re(S_i^a(\tau))}{\pi},$$

$$\int D\mu = C_M \prod_{\tau} \int_{-i\infty}^{i\infty} \frac{\varepsilon d\mu(\tau)}{2\pi i}, \quad (34)$$

involving the constant  $C_M = C^M$  to be fixed below and the action

$$A = \sum_{\tau} d\tau \left\{ \mathbf{S}^*(\tau) \cdot \frac{d\mathbf{S}(\tau)}{d\tau} + \mu(\tau)(\mathbf{S}^*(\tau) \cdot \mathbf{S}(\tau) - Nm\sigma) \right. \\ \left. + H(\mathbf{S}^*(\tau), \mathbf{S}(\tau - d\tau)) \right\}, \quad (35)$$

where  $d\tau \equiv \varepsilon$  and  $d\mathbf{S}(\tau)/d\tau \equiv (\mathbf{S}(\tau) - \mathbf{S}(\tau - d\tau))/d\tau$  involves  $\mathbf{S}(\tau)$  due to Eq. (30) and  $\mathbf{S}(\tau - d\tau)$  due to Eq. (32). The trace structure leads to periodic boundary conditions

$\mathbf{S}(\beta) = \mathbf{S}(0)$ , related to the bosonic nature of the spherical spins. One might be tempted to take the continuum limit of Eq. (33). However, note that this is a dangerous limit since problems can arise that do not occur in our discrete formulation [41]. For a concrete example, we have discussed in Appendix A what is the origin of the problem.

*2.5.1. Free spins in a field*

The simple case of free spherical spins in an external field is already non-trivial [34]. This is because the spherical constraint couples the spins. Let us consider the Hamiltonian

$$H = -\Gamma \sum_i (S_{iop}^{x\dagger} + S_{iop}^x). \tag{36}$$

We can introduce imaginary time Fourier transforms

$$\begin{aligned} \mathbf{S}_i(\tau) &= \sum_{\omega} \mathbf{S}_{i\omega} e^{-i\omega\tau}, \\ \mathbf{S}_{i\omega} &= \frac{1}{M} \sum_{\tau} \mathbf{S}_i(\tau) e^{i\omega\tau}, \end{aligned} \tag{37}$$

where  $\omega = 2\pi nT$  is a Matsubara frequency with  $1 \leq n \leq M$  and  $\tau = j\beta/M$  with  $1 \leq j \leq M$ . Integrating out the spins we obtain

$$Z = \int D\mu \exp(-NA) \tag{38}$$

with (denoting imaginary times again by  $j = \tau/\varepsilon$ ),

$$A = -\varepsilon m \sigma \sum_j \mu(j\varepsilon) + m \text{tr}_j \ln B - \varepsilon^2 \Gamma^2 \sum_{jj'} B_{jj'}^{-1}, \tag{39}$$

where

$$B_{jj'} = (1 + \varepsilon\mu(j\varepsilon))\delta_{jj'} - \delta_{j,j'+1} \tag{40}$$

with  $\delta_{1,M+1} \equiv 1$  due to the periodic boundary condition. We write

$$\mu(j\varepsilon) = \mu + \mu_j(1 + \varepsilon\mu), \tag{41}$$

where  $\mu$  is the saddle-point value, that will turn out to be real, whereas the deviations  $\mu_j$  are imaginary and turn out to be  $\mathcal{O}(N^{-1/2})$ . We expand to second order in  $\mu_j$ . The matrix

$$\bar{B}_{jj'} = \frac{1}{1 + \varepsilon\mu} B_{jj'}(\mu) \tag{42}$$

has diagonal elements 1 and off-diagonal elements  $-a = -1/(1 + \varepsilon\mu)$ . Its inverse is [41]

$$\begin{aligned} \bar{B}_{ij}^{-1} &= \frac{1}{1 - a_\lambda^M} a_\lambda^{i-j}, & i \geq j, \\ &= \frac{1}{1 - a_\lambda^M} a_\lambda^{M+i-j}, & i < j. \end{aligned} \tag{43}$$

We can now expand the action to second order in  $\mu_j$ . This gives after some algebra

$$A = A_0 + A_1 + A_2, \quad (44)$$

$A_0$  is the saddle-point free energy

$$\begin{aligned} \beta F = A_0 &= -\beta_j \mu \sigma + m \ln [(1 + \varepsilon \mu)^M - 1] - \frac{\beta \Gamma^2}{\mu} \\ &\rightarrow -\beta_j \mu \sigma + m \ln [e^{\beta \mu} - 1] - \frac{\beta \Gamma^2}{\bar{\mu}}. \end{aligned} \quad (45)$$

This gives the saddle-point equation

$$\frac{m}{1 - e^{-\beta \mu}} + \frac{\Gamma^2}{\mu^2} = m \sigma. \quad (46)$$

At zero field one has  $e^{\beta \mu} = \sigma/(\sigma - 1)$ , yielding  $\beta F = -S_\infty$  with infinite temperature entropy

$$S_\infty = m[\sigma \ln \sigma - (\sigma - 1) \ln(\sigma - 1)]. \quad (47)$$

Due to the scaling of the spherical constraint with  $m$  and the harmonic nature of the spherical spins, this yields an equal amount of entropy for each spin direction.

For non-zero field the large temperature behavior is still of this form. For small temperatures, however, excitations will have a gap  $\Delta E = \mu(T = 0) = \Gamma/\sqrt{m(\sigma - 1)}$ . This follows since

$$\mu = \frac{\Gamma}{\sqrt{m(\sigma - e^{\beta \mu}/(e^{\beta \mu} - 1))}} \approx \frac{\Gamma}{\sqrt{m(\sigma - 1)}} \left(1 + \frac{e^{-\beta \Delta E}}{2(\sigma - 1)}\right). \quad (48)$$

Note that this gap scales linearly in the field  $\Gamma$ , as expected for free spins in a field. Other quantization schemes have been proposed where the action involved a second-order derivative in imaginary time [42–44]. Physically, this is due to a kinetic term of the form  $(dS/d\tau)^2$  rather than our first-order derivative  $S^* dS/d\tau$  arising from the Trotter approach. The kinetic terms describe different physics, e.g. the quantized kinetic energy of a rotor. Such a system always has a finite-energy gap due to its harmonic oscillator character. Spin systems are fundamentally different. Spins have no kinetic energy, and for quantized spherical spins the energy gap, indeed, vanishes when the field vanishes.

The next terms in Eq. (44) fix the prefactor of the path integral. They are discussed in Appendix B.

### 2.5.2. Pair couplings

Another non-trivial situation is quantized spherical spins that are coupled in pairs in the presence of an external field. This covers both the ferromagnet and the spin-glass cases:

$$H = - \sum_{ij} J_{ij} \mathbf{S}_{i,op}^\dagger \mathbf{S}_{j,op} - \sum_i \Gamma_i (S_{i,op}^{x\dagger} + S_{i,op}^x). \quad (49)$$

We can diagonalize the coupling matrix, and introduce imaginary time Fourier transforms

$$\begin{aligned}
 \mathbf{S}_i(\tau) &= \sum_{\omega} \sum_{\lambda} \mathbf{S}_{i\omega} e_i^{\lambda} e^{-i\omega\tau}, \\
 \mathbf{S}_{i\omega} &= \frac{1}{M} \sum_{i\tau} \mathbf{S}_i(\tau) e^{i\omega\tau} e_i^{\lambda},
 \end{aligned}
 \tag{50}$$

where  $e_i^{\lambda}$  is the normalized eigenvector of  $J_{ij}$  with eigenvalue  $J_{\lambda}$ . Integrating out the spins we obtain the intensive free energy

$$\beta F = -\beta\mu\sigma + mM \ln(1 + \varepsilon\mu) + \frac{1}{N} \sum_{\lambda} \left( m \ln(1 - a_{\lambda}^M) - \frac{Me^2\Gamma_{\lambda}^2}{1 - a_{\lambda}} \right)
 \tag{51}$$

$$\rightarrow -\beta\mu\sigma + m \int \rho(J_{\lambda}) dJ_{\lambda} \ln(e^{\beta\mu} - e^{\beta J_{\lambda}}) - \int \rho(J_{\lambda}) dJ_{\lambda} \frac{\beta\Gamma_{\lambda}^2}{\mu - J_{\lambda}},
 \tag{52}$$

where  $\Gamma_{\lambda} = \sum_i e_i^{\lambda} \Gamma_i$  is the projection of the field on eigenstate  $\lambda$ . The thermally averaged occupation numbers are

$$\langle S_{i\omega}^* S_{i\omega} \rangle = \frac{T}{\mu - i\Omega_{i\omega} - J_{\lambda} e^{i\omega\tau}}.
 \tag{53}$$

These results have been analyzed for a ferromagnet on a simple cubic lattice. One has  $J_{\lambda} \rightarrow J(k) = 2J(\cos k_x + \cos k_y + \cos k_z)$ , with integration measure  $d^3k/(2\pi)^3$ . In particular, one finds a low-temperature specific heat  $C \sim mT^{3/2}$  due to spin waves in  $m$ -directions. Note that the spherical constraint also allows longitudinal spin waves [34].

When spins are only coupled in the  $z$ -direction, while the field acts in the transverse ( $x$ ) direction, one has in the limit  $M \rightarrow \infty$

$$\beta F = -\beta\mu\sigma + \int \frac{d^3k}{(2\pi)^3} \ln(e^{\beta\mu} - e^{\beta J(k)}) + (m - 1) \ln(e^{\beta\mu} - 1) - \frac{\beta\Gamma^2}{\mu - 6J}.
 \tag{54}$$

From these equations the zero-temperature quantum-phase transition in a transverse field can be analyzed. Some results were given in Ref. [34].

The case of a spherical spin glass with pair couplings between the  $z$ -components will be useful for a check of the results of next section. Here  $J_{ij}$  are random Gaussian with average zero and variance  $J^2/N$ . The distribution of eigenvalues is the semi-spherical law

$$\rho(J_{\lambda}) = \frac{1}{2\pi J^2} \sqrt{4J^2 - J_{\lambda}^2}
 \tag{55}$$

with  $-2J < J_i < 2J$ . For any  $M$  one can now calculate the thermal occupation numbers

$$\begin{aligned}\hat{q}_{d\omega} &= \int \rho(J_i) dJ_i \langle S_{i\omega}^* S_{i\omega} \rangle \\ &= \int \rho(J_i) dJ_i \frac{T}{\mu - i\Omega_{\omega} - J_i e^{i\omega}} \\ &= \frac{2T}{\mu - i\Omega_{\omega} + \sqrt{(\mu - i\Omega_{\omega})^2 - 4J^2 e^{2i\omega}}}.\end{aligned}\quad (56)$$

Below the phase transition the system will have condensed partly in the mode with largest eigenvalue  $2J$ . Its occupation number  $Nq \equiv S_{2J}^* S_{2J}$  will be extensive. For  $\omega = 0$  one then has the expectation value

$$\tilde{q} \equiv \hat{q}_{d\omega=0} = q + \frac{2T}{\mu + \sqrt{\mu^2 - 4J^2}}.\quad (57)$$

The free energy reads

$$\begin{aligned}\beta F &= -\beta\mu m\sigma + \int \rho(J_i) dJ_i \times \sum_{\omega} \ln(1 + \varepsilon\mu - (1 + \varepsilon J_i) e^{2i\omega}) \\ &\quad + (m-1) \sum_{\omega} \ln(1 + \varepsilon\mu - e^{2i\omega}) - \frac{\beta\Gamma^2}{\mu} + \beta(\mu - 2J)q,\end{aligned}\quad (58)$$

where the  $(m-1)$ -terms arise from the transverse spin components and the last term from the ordering field, respectively. Using

$$\int \rho(J_i) dJ_i \ln(a - bJ_i) = \ln \frac{a + \sqrt{a^2 - 4b^2}}{2} + \frac{a - \sqrt{a^2 - 4b^2}}{2(a + \sqrt{a^2 - 4b^2})}\quad (59)$$

for  $a = 1 + \varepsilon\mu - e^{2i\omega}$ ,  $b = \varepsilon e^{2i\omega}$ , we can express the integral as

$$\begin{aligned}-1 + \beta\mu(\tilde{q}_d - q) - \ln(M(\tilde{q}_d - q)) - \frac{\beta^2 J^2}{2} (\tilde{q}_d - q)^2 \\ + \sum_{\omega \neq 0} [-1 + \beta(\mu - i\Omega_{\omega})\hat{q}_{d\omega} - \ln(M\hat{q}_{d\omega}) - \frac{\beta^2 J^2}{2} e^{2i\omega} \hat{q}_{d\omega}^2].\end{aligned}\quad (60)$$

Variation of Eq. (58) w.r.t.  $S_{2J}$  yields  $q \equiv S_{2J}^* S_{2J}/N = 0$  or  $\mu = 2J$ ,  $q > 0$ . In the latter case Eq. (57) yields  $\tilde{q}_d = q + T/J$ . We may therefore make the replacement

$$-2\beta Jq + \beta J\tilde{q}_d q - \frac{\beta^2 J^2}{2} q^2 \rightarrow \frac{\beta^2 J^2}{2} q^2 - \frac{q}{\tilde{q}_d - q}.\quad (61)$$

This finally leads to

$$\begin{aligned} \beta F = & -\frac{\beta^2 J^2}{2}(\tilde{q}_d^2 - q^2) - \frac{q}{\tilde{q}_d - q} - 1 + \beta\mu(\tilde{q}_d - m\sigma) \\ & - \ln \left[ \beta\mu(\tilde{q}_d - q) - \frac{\beta\Gamma^2}{\mu} + m \ln[(1 + \varepsilon\mu)^M - 1] \right] \\ & + \sum_{\omega \neq 0} \left[ -1 + \beta(\mu - i\Omega_\omega)\hat{q}_{d\omega} - \ln(\beta(\mu - i\Omega_\omega)\hat{q}_{d\omega}) \right. \\ & \left. - \frac{\beta^2 J^2}{2} e^{2i\varepsilon\omega} \hat{q}_{d\omega}^2 \right]. \end{aligned} \tag{62}$$

In the next section we shall recover this expression as the  $p = 2, x \rightarrow 0$  case of Eqs. (65) and (67). The condition  $x = 0$  occurs due to absence of replica symmetry breaking. This should be expected since the system condenses in only one mode, the one having the largest eigenvalue [45]. When also short-range ferromagnetic interactions are present, thermodynamics and correlation functions can be solved exactly. The largest mode may then be due to the onset of spin-glass ordering or of ferromagnetism [46].

For low  $T$  the representation, Eq. (51), shows that the specific heat behaves as  $T^{3/2}$ . One can also determine the time-dependent correlation function

$$\begin{aligned} q_d(\tau) = & \sum_{\omega} \hat{q}_{d\omega} e^{i\omega\tau} \\ = & \int \rho(J_i) dJ_i \frac{e^{\tau(\mu - \lambda)}}{1 - e^{-\beta(\mu - \lambda)}} \quad (-\beta < \tau \leq 0). \end{aligned} \tag{63}$$

At  $T = 0$  it is unity in  $\tau = 0$  and zero in  $0^+$ , while it decays as  $q_d(\tau) \sim |\tau|^{-3/2}$  for  $\tau \rightarrow -\infty$ .

### 2.6. Spin glass in a transverse field

It is known that a given classical Hamiltonian may come from several quantum Hamiltonians. A similar situation occurs here. The simplest case is where the classical Hamiltonian contains complex-valued spins [47], which can be replaced by operators. We thus consider the case where  $H$  depends at each site either on the creation or the annihilation operator. For  $p = 4$  we have the Hamiltonian

$$\begin{aligned} H = & \frac{-1}{4!} \sum_{i,j,k,l=1}^N J_{ijkl} S_{iop}^z S_{jop}^{z\dagger} S_{kop}^z S_{lop}^z \\ & - \Gamma \sum_i (S_{iop}^{x\dagger} + S_{iop}^x) \end{aligned} \tag{64}$$

with Hermitean  $J_{ijkl}$  [47]. (For odd  $p$  we have to add Hermitean conjugate terms; here they are included already.) This means that for each quartet  $(i, j, k, l)$  with  $i < j, k < l$

there are four independent random variables,  $J'_{1,2}$  and  $J''_{1,2}$ , each having average zero and variance  $9J^2/N^5$ . In terms of  $J_{1,2} = J'_{1,2} + iJ''_{1,2}$  the couplings in Eq. (64) read  $J_{ijkl} = J_{klij}^* = J_1 + iJ_2$  and  $J_{ilkj} = J_{kjil}^* = J_1 - iJ_2$ . These results hold for  $i < j, k < l$ . The other sectors follow, of course, by symmetry:  $J_{ijkl} = J_{jikl} = J_{ijlk} = J_{jilk}$ . A similar approach will work for general even  $p$ .

In the replicated free energy, we look for a saddle point with  $\mu_x(\tau) = \mu$  and  $q_{\alpha\alpha}(\tau, \tau') = \langle S_x^\alpha(\tau)^* S_x^\alpha(\tau') \rangle = q_d(\tau - \tau')$  and with  $q_{\alpha\beta}(\tau, \tau') = \langle S_x^\alpha(\tau)^* S_x^\beta(\tau') \rangle = q_{\alpha\beta}$  independent of  $\tau, \tau'$  for  $\alpha \neq \beta$ . For  $M$  Trotter steps the free energy for a one step replica symmetry-breaking solution with plateau  $q$  and breakpoint  $x = 1 - \xi$  reads

$$F = F_{static} + F_{quant} \quad (65)$$

with

$$\begin{aligned} \beta F_{static} = & -\frac{\beta^2 J^2}{2} (\tilde{q}_d^p - \xi q^p) - \frac{1}{x} \ln \frac{\tilde{q}_d - \xi q}{\tilde{q}_d - q} - 1 \\ & + \beta \mu (\tilde{q}_d - m\sigma) - \ln[\beta \mu (\tilde{q}_d - q)] - \frac{\beta \Gamma^2}{\mu} + m \ln[e^{\beta \mu} - 1] \end{aligned} \quad (66)$$

being mainly twice as large as  $F_{classic}$  in Eq. (5), due to doubling of spin degrees of freedom (now complex, previously real). A more important difference is the replacement  $m \ln \beta \mu \rightarrow m \ln(e^{\beta \mu} - 1)$ . As we shall see, this improves quite a bit on the not-too-low-temperature behavior. After deriving this expression at finite  $M$  we have replaced a term  $m \ln[(1 + \varepsilon \mu)^M - 1]$  (see also Eq. (62)), by its limit  $m \ln[e^{\beta \mu} - 1]$ ; we shall come back to this point below. The quantum correction reads at finite  $M$

$$\begin{aligned} \beta F_{quant} &= \sum_{\omega \neq 0} [-1 + \beta(\mu - i\Omega_\omega) \hat{q}_{d\omega} - \ln(\beta(\mu - i\Omega_\omega) \hat{q}_{d\omega})] \\ &\quad - \frac{\beta^2 J^2}{2M} \sum_{\tau} q_d^{p/2}(\varepsilon + \tau) q_d^{p/2}(\varepsilon - \tau) + \frac{\beta^2 J^2}{2} \tilde{q}_d^p. \end{aligned} \quad (67)$$

Here we have Fourier transforms

$$q_d(\tau) = \sum_{\omega} \hat{q}_{d\omega} e^{i\omega\tau}, \quad \hat{q}_{d\omega} = \frac{1}{M} \sum_{\tau} q_d(\tau) e^{-i\omega\tau} \quad (68)$$

and denoted  $\tilde{q}_d \equiv \hat{q}_{d\omega=0}$ .

If one inserts in the  $J^2$  term of  $F_{quant}$  that  $q_d(\tau) = \tilde{q}_d$  is independent of  $\tau$ , the  $J^2$ -terms cancel. Then the  $q_\omega$ 's can be solved, after which the whole  $F_{quant}$  vanishes identically. This is closely related to the static approximation (SA) of Ising models (see below) introduced by Bray and Moore [22]. This approximation neglects the time dependence of the correlator  $q_d(\tau)$  where  $q_d(\tau) \rightarrow q_d$  is also independent of  $\tau$ . The remaining difference with previous classical theory is the replacement  $m \ln \beta \mu \rightarrow m \ln(\exp(\beta \mu) - 1)$  i.e. going from  $2F_{classic}$  to  $F_{static}$ . This replacement already improves

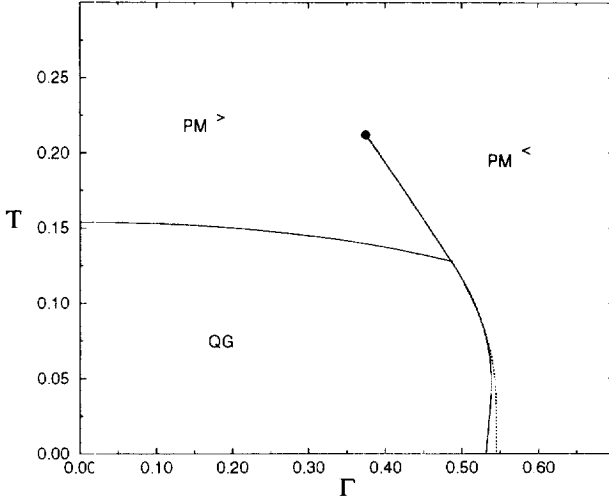


Fig. 3. Phase diagram for the quantum spherical model for  $p = 4$ . The multicritical point and the critical point are given in the static approximation (SA) by  $T_{mcp} = 0.12781, \Gamma_{mcp} = 0.486, T_{cep} = 0.2118, \Gamma_{cep} = 0.3743$ . The continuous line is the SA and the dotted line is the  $M \rightarrow \infty$  extrapolation which yields  $\Gamma_c = 0.5453$  at  $T = 0$ .

the low-temperature behavior. The phase diagram in the SA can be numerically computed and is shown in Fig. 3. It is qualitatively similar to that computed in the classical case (see Fig. 1). We find a thermodynamically first-order transition line with a multi-critical point terminating in the high- $T$  phase in a critical end point. At low temperatures the first-order line shows the phenomena of reentrance and negative latent heat along that line down to  $T = 0$ . This is a failure of the SA as we will show below.

Beyond the static approximation the saddle-point equations read

$$\frac{\hat{c}}{\hat{c}\mu} = 0 \rightarrow q_d(\beta) + \frac{\Gamma^2}{\mu^2} + (m-1) \frac{e^{\beta\mu}}{e^{\beta\mu} - 1} = m\sigma, \tag{69}$$

$$\begin{aligned} \frac{\hat{c}}{\hat{c}\tilde{q}_d} = 0 \rightarrow \beta\mu = & \frac{1}{\tilde{q}_d - q} - \frac{p\beta^2 J^2}{2} q^{p-1} \\ & + \frac{p\beta^2 J^2}{2M} \sum_{\tau} q_d^{p/2-1} (\varepsilon - \tau) q_d^{p/2} (\varepsilon + \tau), \end{aligned} \tag{70}$$

$$\frac{\hat{c}}{\hat{c}q} = 0 \rightarrow \frac{p\beta^2 J^2}{2} q^{p-1} = \frac{q}{(\tilde{q}_d - q)(\tilde{q}_d - \xi q)}, \tag{71}$$

$$\frac{\hat{c}}{\hat{c}x} = 0 \rightarrow -\frac{\beta^2 J^2}{2} q^p + \frac{1}{x^2} \ln \frac{\tilde{q}_d - \xi q}{\tilde{q}_d - q} - \frac{q}{x(\tilde{q}_d - \xi q)} = 0. \tag{72}$$

The latter equation is solved by  $x = (p-1-\eta)(\tilde{q}_d - q)/(\eta q)$  with the same  $\eta$  as in the classical case Eq. (12).

Both for  $\omega \neq 0$  and for  $\omega = 0$  we multiply  $\partial F_{\text{quant}} / \partial \hat{q}_{d\omega}$  by  $\hat{q}_{d\omega}$  and go to the time domain. This yields

$$\begin{aligned} & \beta\mu q_d(\tau) + M(q_d(\tau) - q_d(\tau + \varepsilon)) \\ &= M\delta_{\tau,\beta} - \frac{\xi q^2}{(\tilde{q}_d - q)(\tilde{q}_d - \xi q)} \\ &+ \frac{p\beta^2 J^2}{2M} \sum_{\tau'} q_d(\tau + \varepsilon - \tau') q_d^{p/2-1}(\varepsilon - \tau') q_d^{p/2}(\varepsilon + \tau') \end{aligned} \quad (73)$$

with  $\tau = j\varepsilon$ ,  $j = 1, 2, \dots, M$ , and  $\varepsilon = \beta/M$ . Note that now Eq. (70) becomes redundant, as it follows already by summing Eq. (73) over  $\tau$ .

### 2.6.1. Numerical solution at finite $M$

We have numerically studied the quantum equations with  $m = \sigma = 2$ . In order to compare with the classical case where  $(1/N) \sum S_i^2 = 1$ , we have rescaled spins  $S \rightarrow S/\sqrt{m\sigma}$ ,  $S^* \rightarrow S^*/\sqrt{m\sigma}$  to yield a unit constraint also in the quantum case. This amounts to scaling temperatures and fields to  $T \rightarrow T/(m\sigma)^2$ ,  $\Gamma \rightarrow \Gamma/(m\sigma)^{3/2}$ .

The Trotter limit  $M \rightarrow \infty$  should be taken. This set of non-linear equations can be numerically solved for a different values of  $M$ . We find that depending on the regularization term [48] we use for the static part of the free energy eq. Eq. (66) the low-temperature behavior of the first-order line shows quite strong finite  $M$  corrections and the numerical extrapolation to the limit  $M \rightarrow \infty$  is not safe. To overcome this problem we did the following: we took two different regularizations for  $F_{\text{static}}$ , i.e. we replaced the term  $m \log(e^{\beta\mu} - 1)$  by the general  $m_1$  dependent expression

$$(m - m_1) \log(e^{\beta\mu} - 1) + m_1 \log \left( \left( 1 + \frac{\beta\mu}{M} \right)^M - 1 \right). \quad (74)$$

Note that in the limit  $M \rightarrow \infty$  this expression coincides with the term  $m \log(e^{\beta\mu} - 1)$  for any value of  $m_1$ . For finite  $M$  the behavior of the first-order transition line at very low temperatures strongly depends on the value of  $M$ . This is a direct consequence of the correct order of limits in the saddle point equations where the limit  $M \rightarrow \infty$  should be taken before the limit  $T \rightarrow 0$ . Consequently, the behavior of the line in the limit  $T \rightarrow 0$  is quite different if these limits are taken in the opposite way (i.e. first,  $T \rightarrow 0$  and later on  $M \rightarrow \infty$ ).

In the classical model we had  $M = 1$ ,  $m_1 = m$ . We found that the first-order line matches the  $T = 0$  axis with a negative slope without reentrance (see Fig. 1). In the quantum case with  $m_1 = 1$ ,  $M \geq 1$  this situation persists with smaller value for  $\Gamma$  at  $T = 0$  and larger slope of the transition line. In the static approximation (Eq. (66)) one has  $m_1 = 0$ , so the regularization term coincides with the  $M \rightarrow \infty$  limit itself. In this case the model shows the phenomena of reentrance for finite  $M$  close to zero temperature (like in the SA of the Ising model, see below). As we expect the transition line to have infinite slope, this indicates that for each  $M$  an optimal value for  $m_1$  exists between 0 and 1 where the slope is infinite.

Numerically, we proceed in the following way: for a given value of  $M$  we determined the value of  $m_1$  such that the first-order transition line meets the  $T = 0$  axis with infinite slope. The *optimal* lines obtained in this way for different values of  $M$  (we took  $M = 1, 3, 5, 7, 9, 11, 21, 41$ ) are then extrapolated to  $M \rightarrow \infty$ . We found that a second degree polynomial in  $1/M$  is enough for such extrapolation to be accurate (even if higher-order polynomials are needed at very low temperatures).

At zero temperature we obtain  $\Gamma_c = 0.5453$  for  $p = 4$  and  $m_1 \simeq 0.033$ . The resulting extrapolated boundary line for  $p = 4$  is depicted in Fig. 3. Only at very low-temperatures deviations from the SA are important. The phenomena of reentrance has now disappeared since this was an artifact of the SA. The latent heat at very low temperatures, across the first-order transition line, vanishes exponentially with  $1/T$ . At high-temperatures corrections to the SA are, indeed, very small and the value of the transition field in the SA, is always larger than the exact  $M \rightarrow \infty$  extrapolated value. The opposite result is found at very low temperatures.

In Section 3 we will see that a similar scenario is valid for Ising spins in the SA and also beyond it.

2.6.2. *Continuum limit:  $M \rightarrow \infty$*

Let us now take the limit  $M \rightarrow \infty$ . We set

$$q_d(\tau) = q + p(\tau) \tag{75}$$

with  $p(\tau) = p(\tau + \beta)$ . Eq. (73) implies a discontinuity for  $\tau = 0^+$ :  $p(0^+) = p(0) - 1$  with  $p$  being left-continuous at 0. At other  $\tau$  one gets

$$\begin{aligned} \frac{dp(\tau)}{d\tau} &= \frac{p(\tau)}{\int d\tau' p(\tau')} + \frac{pJ^2}{2} \int_{-\beta/2}^{\beta/2} d\tau' [p(\tau) - p(\tau + \tau')] \\ &\quad \times [(q + p(\tau'))^{p/2-1} (q + p(-\tau'))^{p/2} - q^{p-1}]. \end{aligned} \tag{76}$$

Further, one has

$$q + p(0) + \frac{\Gamma^2}{\mu^2} + \frac{m-1}{1 - e^{-\beta\mu}} = m\sigma, \tag{77}$$

$$\frac{p(p-1)J^2}{2} q^{p-1} = \frac{\eta q}{(\int d\tau p(\tau))^2}, \tag{78}$$

$$\begin{aligned} \mu &= \frac{1}{\int d\tau' p(\tau')} \\ &+ \frac{pJ^2}{2} \int_{-\beta/2}^{\beta/2} d\tau' [(q + p(\tau'))^{p/2-1} (q + p(-\tau'))^{p/2} - q^{p-1}]. \end{aligned} \tag{79}$$

The internal energy reads

$$U = - \int_{-\beta/2}^{\beta/2} d\tau [(q + p(\tau))^{p/2} (q + p(-\tau))^{p/2} - q^p] - \frac{(p-1-\eta)q^{p-1}}{\eta} \int_{-\beta/2}^{\beta/2} d\tau p(\tau) - \frac{2\Gamma^2}{\mu}. \quad (80)$$

For  $p = 4$  its Fourier representation reads

$$U = -\beta J^2 \sum_{\omega_1 + \omega_2 = \omega_3 + \omega_4} \hat{q}_{d\omega_1} \hat{q}_{d\omega_2} \hat{q}_{d\omega_3} \hat{q}_{d\omega_4} + \beta J^2 q^4 - \frac{(p-1-\eta)q^{p-1}}{n} \beta p_{\omega=0} - \frac{2\Gamma^2}{\mu}, \quad (81)$$

where  $\hat{q}_{d\omega} = p_{\omega} + q\delta_{\omega,0}$ .

These equations are particularly useful at  $T = 0$ . It can then be seen that  $p(\tau) \sim 1/\tau^2$  for  $\tau \rightarrow \pm\infty$ , implying that  $p_{\omega} = T \int d\tau p(\tau) e^{i\omega\tau} \sim T(1 + |\omega| + i\omega)$ . Expanding the sums in Eq. (81) in powers of  $p$  we find sums over 1, 2, and 3 frequencies. The one-frequency sum can be calculated as follows. We extend the Euler–Maclaurin formula to complex functions with non-analyticities of the form  $|\omega|$ , and obtain

$$T \sum_{\omega=2\pi nT} f_{\omega} = \int \frac{d\omega}{2\pi} f(\omega) - \frac{2\pi T^2}{6} \Re \left. \frac{df}{d\omega} \right|_{0-}. \quad (82)$$

The two and three frequency sums are convolutions of this and produce also  $T^0 + T^2$  terms. This yields a behavior  $U = U_0 + U_2 T^2$ , which implies a linear specific heat,  $C \approx 2U_2 T$ , in the spin-glass phase. This result holds for the present  $p$ -spin model. Unlike stated previously [47],  $C \sim T$  also holds for the  $p = 2 + 4$  model with infinite replica symmetry breaking. For  $p = 2$  only there is no replica symmetry breaking, and the system is in another universality class. As discussed above, one then has  $C \sim T^{3/2}$ .

### 3. Ising spins

The Ising  $p$  spin-glass model in a transverse field is defined by

$$\mathcal{H} = - \sum_{i_1 < i_2 < \dots < i_p} J_{i_1 i_2 \dots i_p} \sigma_{i_1}^z \sigma_{i_2}^z \dots \sigma_{i_p}^z - \Gamma \sum_i \sigma_i^x, \quad (83)$$

where  $\sigma_i^z, \sigma_i^x$  are the Pauli spin matrices and  $\Gamma$  is the transverse field. The indices  $i_1, i_2, \dots, i_p$  run from 1 to  $N$  where  $N$  is the number of sites. The  $J_{i_1 i_2 \dots i_p}$  are couplings Gaussian distributed with zero mean and variance  $p!J^2/(2N^{p-1})$ . We shall choose units in which  $J = 1$ .

Here we will compute in the SA, the phase diagram of the model Eq. (83) and show that coincides in its essentials with that reported in the previous sections. Detailed computations of the quantum Ising model Eq. (83) have been already presented in the literature. Here we only sketch the main steps of the derivation of the saddle-point equations skipping the details. The interested reader will find more details about their derivation in Refs. [28,31,32].

The free energy of the model is computed using the replica method as in the previous section. After discretizing the imaginary time direction using the Trotter–Suzuki decomposition we obtain a problem described by an effective Hamiltonian

$$\mathcal{H}_{\text{eff}} = A \sum_{i < j} J_{ij} \sum_t \sigma_i^t \sigma_j^t + B \sum_{it} \sigma_i^t \sigma_i^{t+1} + C, \tag{84}$$

where the time index  $t$  runs from 1 to  $M$  and the spins  $\sigma_i^t$  take the values  $\pm 1$ . The constants  $A$ ,  $B$  and  $C$  are given by  $A = \beta/M$ ;  $B = \frac{1}{2} \ln(\coth(\beta\Gamma/M))$ ;  $C = (MN/2) \ln(\frac{1}{2} \sinh(2\beta\Gamma/M))$ . Now, we apply the replica trick and compute the average over the disorder of the replicated partition function

$$\overline{Z^n} = \int [dJ] \sum_{\{\sigma_i^t\}} \exp \left( \sum_{a=1}^n \mathcal{H}_{\text{eff}}^a \right). \tag{85}$$

Computations are easily done and the problem can be reduced to a dynamical equation involving Ising spins in a one-dimensional chain. The free energy reads

$$\beta f = \lim_{n \rightarrow 0} \frac{F(Q, A)}{n}, \tag{86}$$

where

$$F(Q, A) = -\frac{nC}{N} + \frac{1}{M^2} \text{Tr}(QA) - \frac{A^2}{2} \sum_{abtt'} (Q_{ab}^{tt'})^p - \ln(H(A)) \tag{87}$$

with  $Q_{ab}^{tt'}$ ,  $A_{ab}^{tt'}$  being the order parameter and the trace  $\text{Tr}$  is done over the replica and time indices. The term  $H(A)$  is given by

$$H(A) = \sum_{\sigma} \exp \left( \sum_{ab} \frac{1}{M^2} \sum_{tt'} A_{ab}^{tt'} \sigma_a^t \sigma_b^{t'} + B \sum_{at} \sigma_a^t \sigma_a^{t+1} \right). \tag{88}$$

The most general time translation-invariant solution of these equations is given by

$$Q_{ab}^{tt'} = Q_{ab} \quad (a \neq b), \quad A_{ab}^{tt'} = A_{ab} \quad (a \neq b), \tag{89}$$

$$Q_{aa}^{tt'} = q_d(t - t'), \quad A_{aa}^{tt'} = \lambda_d(t - t'). \tag{90}$$

Because at zero transverse field the classical solution is a one step of replica symmetry breaking we look also for solutions of this type in the quantum case. We divide the  $n$  replicas into  $n/m$  boxes  $K$  of size  $m$  such that  $m$  divides  $n$ . The saddle-point solution when  $a \neq b$  takes the form  $Q_{ab}^{tt'} = q$ ;  $A_{ab}^{tt'} = \lambda$  if  $a, b \in K$  and  $Q_{ab}^{tt'} = A_{ab}^{tt'} = 0$

otherwise. If  $a = b$  we have  $Q_{aa}^{t''} = q_d(t - t')$ ,  $A_{aa}^{t''} = \lambda_d(t - t')$ . Finally, the free energy reads

$$\begin{aligned} \beta f = & -C - \frac{\beta^2}{4}(m-1)q^p - \frac{\beta^2}{4M^2} \sum_{u'} (q_d(t-t'))^p \\ & + \frac{\beta^2(m-1)}{2}q\lambda + \frac{\beta^2}{2M^2} \sum_{u'} q_d(t-t')\lambda(t-t') \\ & - \frac{1}{m} \ln \left( \int_{-\infty}^{\infty} dp_x \Xi^m(x) \right) \end{aligned} \quad (91)$$

and  $dp_x = dx \exp(-x^2)/(2\pi)^{1/2}$  is the Gaussian measure. The order parameters are determined by solving the saddle-point equations

$$\frac{\partial f}{\partial q} = \frac{\partial f}{\partial \lambda} = \frac{\partial f}{\partial m} = 0, \quad (92)$$

$$\frac{\partial f}{\partial q_d(t-t')} = \frac{\partial f}{\partial \lambda_d(t-t')} = 0, \quad (93)$$

where  $\Xi(x)$  is given by

$$\Xi(x) = \sum_{\{\sigma_i\}} \exp(\Theta(x, \{\sigma_i\})) \quad (94)$$

with

$$\begin{aligned} \Theta(x, \{\sigma_i\}) = & \frac{A^2}{2} \sum_{u'} (\lambda_d(t-t') - \lambda) \sigma_i \sigma_{u'} \\ & + B \sum_i \sigma_i \sigma_{i+1} + A\sqrt{\lambda} x \sum_i \sigma_i. \end{aligned} \quad (95)$$

Solving Eqs. (92) and (93) we get

$$\lambda = \frac{p}{2} q^{p-1}, \quad \lambda_d(t-t') = \frac{p}{2} (q_d(t-t'))^{p-1}, \quad (96)$$

$$q = \langle\langle (\bar{\sigma}_i)^2 \rangle\rangle, \quad q_d(t-t') = \langle\langle \bar{\sigma}_i \bar{\sigma}_{i'} \rangle\rangle, \quad (97)$$

$$\begin{aligned} \frac{(1-p)\beta^2 q^p}{4} = & \frac{1}{m^2} \ln \left( \int_{-\infty}^{\infty} dp_x \Xi^m(x) \right) \\ & - \frac{1}{m} \langle\langle \ln(\Xi(x)) \rangle\rangle, \end{aligned} \quad (98)$$

where the averages  $\langle\langle \dots \rangle\rangle$  and  $\overline{(\cdot)}$  are defined by

$$\langle\langle A(x) \rangle\rangle = \frac{\int_{-\infty}^{\infty} dp_x \Xi(x)^m A(x)}{\int_{-\infty}^{\infty} dp_x \Xi(x)^m}, \quad (99)$$

$$\overline{B(\{\sigma_t\})} = \frac{\sum_{\{\sigma_t\}} B(\sigma_t) \exp(\Theta(x, \{\sigma_t\}))}{\Xi(x)}, \quad (100)$$

where  $\Theta(x, \{\sigma_t\})$  is given in Eq. (95).

The solution of this system of coupled equations is quite complex because there is an infinity of parameters ( $q_d(t-t')$ ) which needs to be computed in a self-consistent way. For  $p=2$  (the SK model in a transverse field) the transition is continuous in the presence of the transverse field and there is only one quantum paramagnetic phase. For  $p=2$  these equations have been studied using five different methods. These are: (1) doing a self-consistent approach [49] or a Ginzburg–Landau expansion [50,51], (2) performing exact small  $M$  calculations [52,53] (3) Perturbative expansions in the field [54,55], (4) numerically solving the Schrödinger equation [56,57] and (5) doing quantum Monte Carlo calculations [58–60]. In the case  $p \geq 3$ , the transition is discontinuous and Eqs. (97) and (98) have been perturbatively solved by expanding around the  $p \rightarrow \infty$  limit [31,32] where the SA (see below) is exact. Here we will revisit the SA showing that the phase diagram of the model coincides in its essentials with that presented previously for the spherical model. We will go beyond the SA later on and numerically solve Eqs. (96)–(98) by doing finite  $M$  calculations in order to check the reliability of that approximation.

### 3.1. Zeroth-order solution: The static approximation

The SA amounts to consider  $q_d(t)$  and  $\lambda_d(t)$  independent of  $t$ . This corresponds to suppress quantum fluctuations. This is exact at zero transverse field but it turns out to be inaccurate at finite field and crucial for the thermodynamic properties at zero temperature. The failure of the SA is very clear in case of continuous quantum-phase transitions where the quantum critical point is characterized by the dynamical exponent  $z$ , an exponent which cannot be computed within the SA. The situation is slightly better in first-order quantum-phase transitions where there is no critical point. Hence, there is no divergent correlation length and imaginary time correlation functions can be well approximated by constant values [19]. Generally, this approximation can be the source of pathologies at low temperatures where the third principle of thermodynamics is usually violated. At not too low temperatures we will see that this approximation yields a phase diagram in qualitative and quantitative agreement (within 10% in the worst case  $p=3$ ) with the full dynamical solution.

Let us first analyze the solution of the mean-field equations in this approximation and study the phase diagram of the model.

Introducing  $\lambda_d(t - t') = \lambda_d$ ,  $q_d(t - t') = q_d$  in the free energy Eq. (91) we get

$$\beta f = \frac{\beta^2(1-m)}{4} - \frac{1}{4}\beta^2 q_d^p - \frac{\beta^2(1-m)q\lambda}{2} - \ln(2) - \frac{1}{m} \ln \int dp_x (\Xi(x))^m, \quad (101)$$

where

$$\Xi(x) = \int_{-\infty}^{\infty} dT_z \cosh(T(x, z)), \quad (102)$$

$$T(x, z) = (b^2 + \beta^2 \Gamma^2)^{1/2}. \quad (103)$$

The  $\lambda, \lambda_d, m$  are determined by solving previous equations Eqs. (96)–(98) and  $q, q_d$  are determined by solving the following equations [61]:

$$q = \langle\langle (\sinh(T)b/T)^2 \rangle\rangle, \quad (104)$$

$$q_d = \langle\langle (\cosh(T)(b/T)^2 + (\beta^2 \Gamma^2 \sinh(T))/T^3) \rangle\rangle, \quad (105)$$

where the average  $\langle\langle \dots \rangle\rangle$  was previously defined in Eq. (99) and the average  $\overline{(\dots)}$  is given by

$$\overline{B(x, z)} = \frac{\int_{-\infty}^{\infty} dp_z B(x, z)}{\Xi(x)}. \quad (106)$$

The phase diagram of the model can now be computed for any arbitrary value of  $p$ . As in the spherical case we find two different paramagnetic phases. Putting  $q = \lambda = 0$  and  $m = 0$  in Eqs. (104) and (105) they reduce to a single equation

$$q_d = \frac{\int_{-\infty}^{\infty} dp_x x^2 (\sinh(\Phi(x)))/\Phi(x)}{\int_{-\infty}^{\infty} dp_x \cosh(\Phi(x))} \quad (107)$$

with  $\Phi(x) = \sqrt{\beta^2 \Gamma^2 + \beta^2 \lambda_d x^2}$  and  $\lambda_d = pq_d^{p-1}/2$ . This equation can be numerically solved. Like in the spherical case one finds two paramagnetic solutions separated by a first-order transition line with latent heat. Let us call  $QP^>$  and  $QP^<$  the quantum paramagnetic phases associated to the largest and smaller value of  $q_d$ , respectively. The transition line can be constructed using the Maxwell rule. As temperature increases the latent heat decreases. Consequently, the first-order line ends in a critical point  $(\beta_c, \Gamma_c)$  with mean-field critical exponents. The existence of this critical point has been already pointed out by Dobrosavljevic and Thirumalai [31]. We have numerically computed it for several values of  $p$ . Details of these computations are given in the Appendix C. In the infinite  $p$  limit this critical point is pushed up to infinite temperature [28] and its scaling behavior in the large  $p$  limit has been analytically obtained in Ref. [31] finding  $\Gamma_c = 0.7579$ ,  $T_c = 0.2593\sqrt{p}$ .

As temperature is lowered the first-order line finishes in a multicritical point which separates the three phases of the model (two paramagnetic  $QP^>$  and  $QP^<$  and one quantum glass QG). The boundary lines which separate the paramagnetic phases from

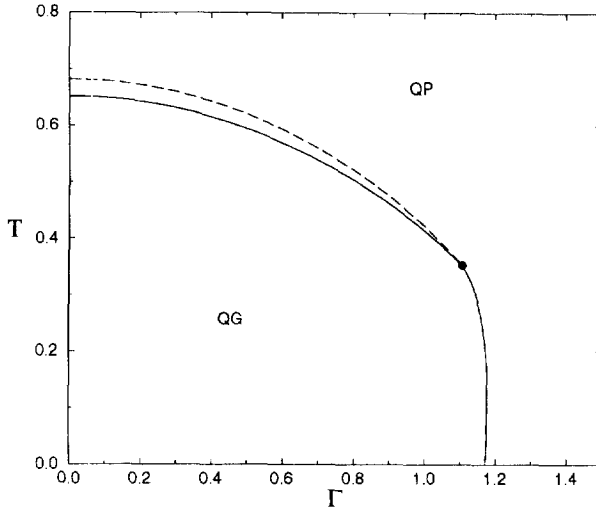


Fig. 4. Phase diagram for  $p = 3$  with Ising spins. The critical point is given by  $T_{cp} = 0.3528, \Gamma_{cp} = 1.1078$ . The multicritical point is extremely close to the critical one and is indistinguishable from it in the figure. At zero temperature,  $\Gamma_c = 1.174$ . The dashed line is the dynamical transition.

the QG phase correspond to different thermodynamic phase transitions. The line which separates  $QP^>$  from QG has no latent heat (this is the continuation of the usual first-order classical phase transition at  $\Gamma = 0$ ). The line which separates  $QP^<$  from QG is a first-order transition with latent heat. The latent heat is positive when crossing the  $QP^< \rightarrow QP^>$  line as well as the  $QP^< \rightarrow QG$  line. Lowering the temperature the  $QP^< \rightarrow QG$  line is determined by the Maxwell construction but allowing  $m$  to be different from 1 and  $q, \lambda$  jump to a higher value when crossing the  $QP^< \rightarrow QG$  line. For low values of  $T$  the breaking point  $m$  is nearly proportional to the temperature and the difference between  $q_d$  and  $q$  proportional to the temperature in the paramagnetic (in this case  $q$  is equal to 0 and  $q_d$  is proportional to  $T$ ) as well as in the quantum-glass side (where  $q$  and  $q_d$  reach a finite value smaller than 1).

The behavior of the latent heat in the boundary lines  $QP^< \rightarrow QP^>$  and  $QP^< \rightarrow QG$  as a function of the temperature is the following: starting from the critical point (where there is no latent heat) and lowering the temperature the latent heat increases as a function of the temperature reaching a maximum in the multicritical point. Then the latent heat decreases and vanishes like  $T^{(p-1)}$  at low temperatures.

We have analyzed in detail the phase diagram for two different values of  $p$ . We have chosen a small ( $p = 3$ ) and a large value of  $p$  ( $p = 10$ ). The phase diagram for  $p = 3$  is shown in Fig. 4 and that of  $p = 10$  is depicted in Fig. 5. The latent heat along the thermodynamic first order transition line is shown in Fig. 6 (for  $p = 3, 10, \infty$  respectively). For sake of completeness we also show the dynamical transition line for different values of  $\Gamma$  in the QP phase (see Refs. [20,21] for more details how this line has been computed in the random orthogonal (ROM) model). The main result

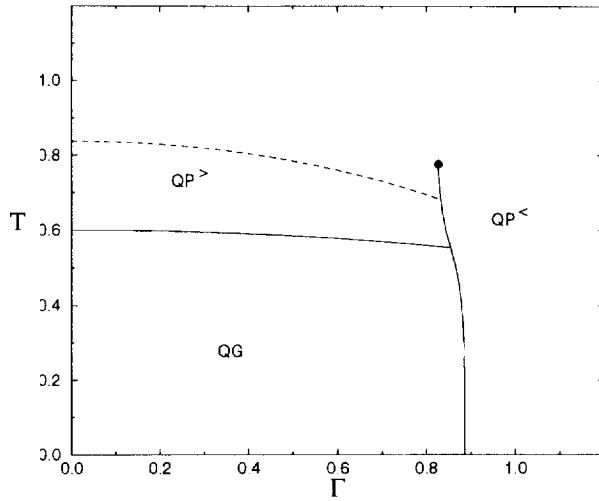


Fig. 5. Phase diagram for  $p = 10$  with Ising spins. The critical point and multicritical point are given by  $T_{cp} = 0.7765$ ,  $\Gamma_{cp} = 0.8903$ ,  $T_{mcp} = 0.5543$ ,  $\Gamma_{mcp} = 0.854$ . At zero temperature  $\Gamma_c = 0.8855$ . The dashed line is the dynamical transition.

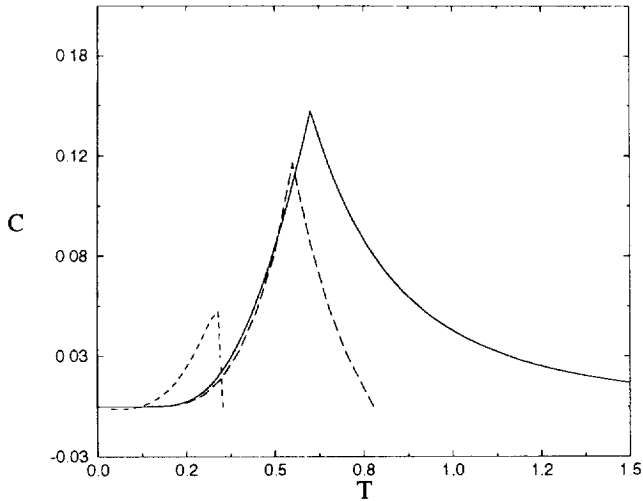


Fig. 6. Latent heat for the  $p$ -spin Ising spin-glass model with  $p = 3, 10, \infty$  (from left to right). The last case are the results obtained by Goldschmidt [28]. It is shown along the boundary lines which separate the  $PM^<$  phase from the other phases as a function of the temperature. There is a maximum at the multicritical point.

concerning this dynamical line is that it crosses the first-order transition  $QP^> - QP^<$  below the ending critical point.

The main difference between Figs. 4 and 5 is that for  $p = 3$  the critical point is hardly observable (but it is there!, the difference between  $T_{cp}$  and  $T_{mcp}$  being of order

$10^{-5}$ ). Also the latent heat corresponding to  $p = 3$  is smaller than that of  $p = 10$ . Being the case  $p = 3$  so close to  $p = 2$  (where the transition is continuous and there is no multicritical point) it is natural to find that the transition is nearly continuous. Note that also for  $p = 3$  the dynamical and the static transition lines are both very close to the multicritical point.

As anticipated in the previous sections we observe in Fig. 6 that the latent heat becomes negative at very low temperatures. For  $p = 3$  this happens below  $T \simeq 0.1$  while for  $p = 10$  this effect persists but is hardly observable. This is a small effect because the latent heat is already of order  $-10^{-3}$  for  $p = 3$  and  $-10^{-5}$  for  $p = 10$ . The same comments presented in the spherical model also apply here. A negative latent heat implies reentrance close to zero temperature. Consider the Clapeyron equation for first-order transition lines  $d\Gamma/dT = L/(T\Delta M_x)$ , where  $L$  is the latent heat and  $\Delta M_x$  is the change in transverse magnetisation when crossing the  $PG^< \rightarrow QG$  line. Because  $\Delta M_x$  is always negative (increasing  $\Gamma$  the transverse ordering  $M_x$  increases) a negative latent heat implies  $d\Gamma/dT > 0$ , i.e. reentrance. In fact, reentrance is observed in Fig. 3 for  $p = 3$  and hardly observable (but there is) in Fig. 4 for  $p = 10$ . In the limit  $p \rightarrow \infty$  reentrance disappears [28]. Like in the case of spherical quantum spins reentrance for finite  $p$  is an artifact of the SA.

Perturbing around  $p=2$  we expect the following scenario for  $p=2$  the transition is continuous (there is no latent heat) and there is no multicritical point. Above a critical value  $p_c^{(1)} \geq 2$  it appears a multicritical point which separates a first-order transition line (with latent heat) from a thermodynamic second-order transition line. The second-order transition line has associated a dynamical transition line (the dynamical transition predicted in the framework of Mode Coupling theories) which meets the static line precisely at the multicritical point.

In the regime  $2 \leq p \leq p_c^{(1)}$  there is a unique quantum paramagnetic phase. Above a given value  $p_c^{(2)}$  such that  $p_c^{(2)} \geq p_c^{(1)}$  a first-order transition line appears with two paramagnetic phases in both sides. Whether  $p_c^{(2)}$  is larger or smaller than 3 is unclear. Within the SA, we expect  $p_c^{(2)}$  to be quite close to 3. A definitive answer to this question requires a full analysis of the theory beyond the SA. In this sense a perturbative study in  $p = 2 + \varepsilon$  would be useful. The fact that  $p = 3$  is close to  $p_c^{(2)}$  explains why the transition looks like a continuous one with very small latent heat (see Fig. 6).

### 3.2. Beyond the static approximation

As said in the previous section it is natural to expect that the SA works well enough if the transition is not continuous. In fact, we expect it should yield better and better results when  $p$  increases (in the  $p \rightarrow \infty$  limit it is exact) even if it is always wrong because it definitely violates the third law of thermodynamics at zero temperature [31]. For smaller values of  $p$  it should be progressively worse being uncontrolled close to the quantum transition point at  $p \simeq p_c^{(2)}$ .

To go beyond the SA we have numerically solved Eqs. (96)–(98) for different values of  $M$  for a fixed value of  $\beta$  and extrapolating the results to the  $M \rightarrow \infty$  limit. This is

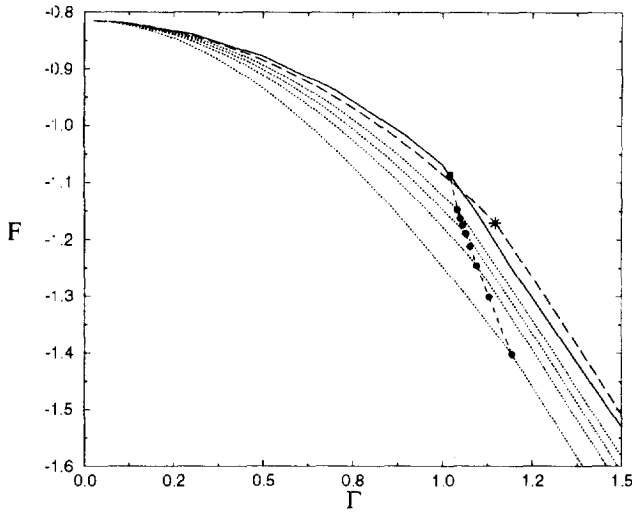


Fig. 7. Free energy as a function of the transverse field  $\Gamma$  in the Ising case for  $p = 3$  and  $T = 0.3$  for different values of  $M$ . The dotted lines correspond (from below to above) to  $M = 4, 6, 8, 12$ . The long-dashed line is the free energy extrapolated to the  $M \rightarrow \infty$  limit. The dashed line which connects the filled circles contains the transition points for different values of  $M$ , the last one is the extrapolated transition in the  $M \rightarrow \infty$  limit. The continuous line is the free energy in the SA and the star indicates the transition point in that approximation.

a method which usually yields good results and has been applied in several cases to continuous quantum-phase transitions in disordered systems [52,53,60]. The essentials of the method has been already presented in Section 3.6 for the spherical quantum model. Here we will show how the method works for first-order quantum-phase transitions in Ising models. Our procedure is quite simple: we solve the system of non-linear equations, Eqs. (96)–(98) for different values of  $M$  looking for a quantum paramagnetic  $\text{QP}^<$  and a quantum glass QG solution. We have used periodic boundary conditions such that  $\sigma_{M+1} = \sigma_1$ . The  $\text{QP}^<$  solution is described by  $q = \lambda = 0$  and  $q_d^{\text{QP}}(t - t')$  different from zero. Without much effort the equations can be solved in the  $\text{QP}^<$  phase up to  $M \simeq 16$ . In the QG phase the solution of the set of non-linear equations requires more computational effort (because  $q, \lambda$  and  $m$  are now finite and some one dimensional integrals cannot be avoided). In this case we were able to solve the equations only up to  $M = 12$ . Looking at the crossing point between the free energies of the two phases we can obtain the transition point for different values of  $M$ . Then we extrapolate the free energies, latent heat as well as the transition point, to the  $M \rightarrow \infty$  limit. A second degree polynomial in  $1/M$  fits quite well the data.

In Figs. 7 and 8 we show the free energy as a function of the transverse field  $\Gamma$  for  $p = 3, T = 0.3$  and  $p = 10, T = 0.4$ . The  $M \rightarrow \infty$  extrapolation is compared to the static ansatz which appears to be a reasonable approximation in this case. The error in predicting the value of the critical field is  $\simeq 10\%$  for  $p = 3$  ( $\Gamma_c^{\text{extra}p} =$

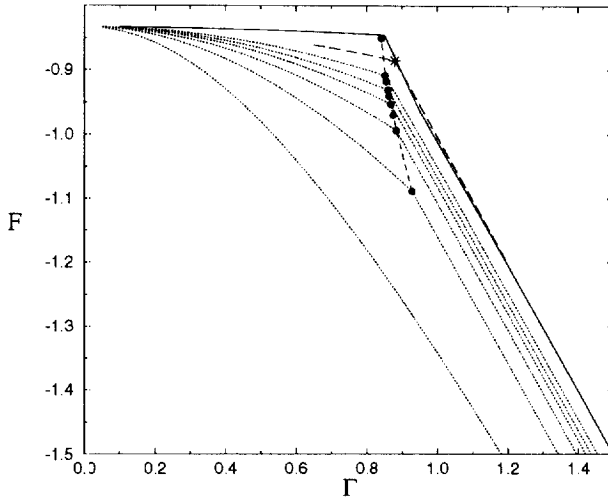


Fig. 8. Free energy as a function of the transverse field  $\Gamma$  in the Ising case for  $p = 10$  and  $T = 0.4$  for different values of  $M$ . The dotted lines correspond (from below to above) to  $M = 2, 4, 6, 8, 10, 14$ . The long-dashed line is the free energy extrapolated to the  $M \rightarrow \infty$  limit. The dashed line which connects the filled circles contains the transition points for different values of  $M$ , the last one is the extrapolated transition in the  $M \rightarrow \infty$  limit. The continuous line is the free energy in the SA and the star indicates the transition point in that approximation.

$1.021 \pm 0.002$ ,  $\Gamma_c^{SA} = 1.14604$ ) and 2% for  $p = 10$  ( $\Gamma_c^{extrap} = 0.841 \pm 0.001$ ,  $\Gamma_c^{SA} = 0.8798$ ). This error should increase at lower temperatures. The latent heat is shown in Fig. 9 for different values of  $M$  as well as the extrapolation to  $M \rightarrow \infty$  compared to the value obtained in the SA. The agreement is very good for  $p = 10$  but not for  $p = 3$  where the SA predicts a latent heat nearly 4 times larger than expected.

Another interesting result in Figs. 7 and 8 concerns the jump in the transverse magnetisation. Using the relation  $\mathcal{M}_x = -\partial F / \partial \Gamma$  this jump manifests in a discontinuous change of the slope of the free energy as a function of  $\Gamma$ . From the figures it can be observed that the transverse magnetisation always decreases going from the QP<sup><</sup> to the QG phase. The jump is very small for  $p = 3$  and increases for larger values of  $p$ .

It is very difficult to perform numerical calculations at much low temperatures, mainly because the scaling behavior in  $M$  is found when the ratio  $\beta/M$  is small in order to extrapolate to the continuum limit  $\beta/M \rightarrow 0$ . At  $T = 0.1$  we have studied the case  $p = 3$  for values  $M = 8, 9, 10, 12, 13, 14$ , this last case being the limit of our computational capabilities. The results are shown in Figs. 9 and 10 where we plot the latent heat as a function of  $1/M$ . It is difficult to extrapolate to  $M \rightarrow \infty$  because we do not have large enough values of  $M$  in order to do that. The data is compatible with the fact that at very low temperatures the latent heat is negligible in the  $M \rightarrow \infty$  limit.

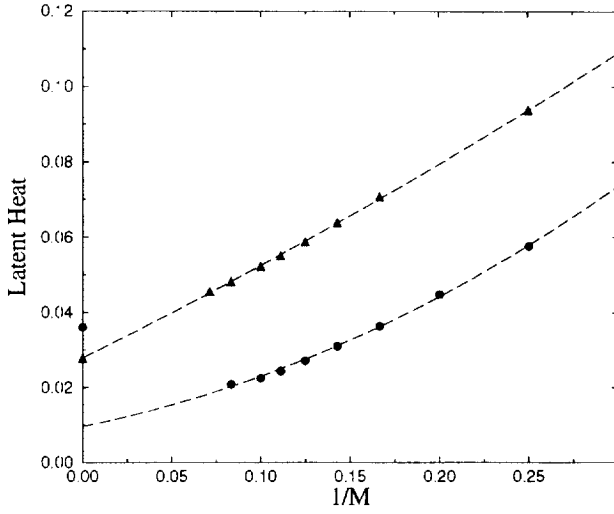


Fig. 9. Latent heat for the Ising case,  $p = 3$  (filled circles) and  $p = 10$  (filled triangles) at the transition point for  $T = 0.3$ ,  $T = 0.4$  respectively as a function of  $1/M$ . The dashed lines are second degree polynomial fits in  $1/M$  to the data. The triangle ( $p = 10$ ) and the circle ( $p = 3$ ) in the vertical axis are the values estimated in the SA ( $L_{p=0}^{extr,p} = 0.027 \pm 0.001$ ,  $L_{p=10}^{SA} = 0.02767$ ,  $L_{p=3}^{extr,p} = 0.0097 \pm 0.001$ ,  $L_{p=3}^{SA} = 0.036$ ).

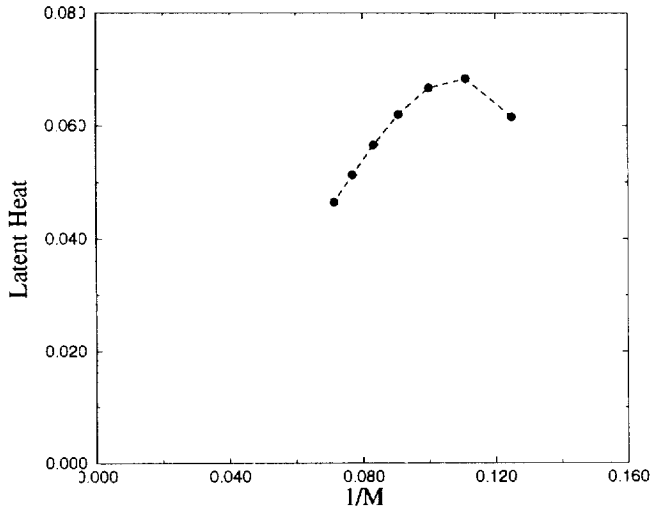


Fig. 10. Latent heat for the Ising case,  $p = 3$  at the transition point for  $T = 0.1$  as a function of  $1/M$ . Extrapolation to the  $M \rightarrow \infty$  limit is not safe since we are far from the scaling region.

#### 4. Discussion and conclusions

In this work we have investigated the quantum-phase transition in spin glasses with multispin interactions in a transverse field. We have introduced a solvable spherical model which yields a phase diagram qualitatively similar to that found in the Ising case (in the static approximation (SA) and also beyond). Details of the quantization of the spherical model have been given. We find indications that the specific heat is linear at low  $T$ . This is possibly related to a finite density of two level systems in the free energy landscape. We have also seen that  $p$ -spin models in a transverse field (spherical and Ising) typically have a first-order transition line in the paramagnet, that we have called the *pre-freezing line*.

For the  $p$ -spin models the study indicates (as expected) that the static approximation (SA) can be considered as a classical approximation where quantum fluctuations are fully neglected. A zero-order calculation shows that the SA seems to yield qualitative good results for first-order (but not too weak) phase transitions at not too low temperatures. The situation is different for continuous quantum-phase transitions. In particular, we have checked the approximate validity of the SA in both the spherical (with quantized spins) and the Ising model numerically computing the free energy and the transition line. This has been done solving the time correlator  $q_d(t - t')$  for finite values of  $M$  and extrapolating to  $M \rightarrow \infty$ . The SA predicts the phase diagram of the model with reasonable accuracy. For instance, for  $p = 3$  in the Ising case the SA yields the phase boundaries with a precision within 10% improving for larger values of  $p$ . The approximate validity of the SA is restricted to high temperatures. Indeed, at very low temperatures the SA fails. This manifests in the phase diagram of both the Ising and spherical cases (this last one with quantized spins) which display the phenomena of reentrance. This pathology is related to the incorrectness of the SA and disappears when taking into account quantum fluctuations.

In the simplest scenario the multicritical point should appear as soon as  $1 \leq p_c^{(1)} < p$ . In this case the phase diagram should be qualitatively similar to that of Fig. 4 with only one quantum paramagnetic phase. Above a second critical value  $p_c^{(2)}$  the multicritical point would develop a line ending in a critical point restoring the two different quantum paramagnetic phases like is observed in Fig. 5. It would be interesting to understand (in the spherical as well as in the Ising cases) how the phase diagram of the model changes when expanding in  $p = 2 + \varepsilon$ . If  $2 < p \leq p_c^{(1)}$  the transition should remain continuous for small  $\varepsilon$ . Then it would be interesting to investigate the dependence (if any) of the dynamical exponent  $z$  with  $\varepsilon$ . Recent results in the ROM model [20,21] suggest that the quantum dynamical exponent could be not universal within mean-field theory. This suggests that models with the same classical behavior may display different quantum behavior in presence of the same type of perturbation.

It would be very interesting to investigate the problem of the existence of more than one quantum paramagnetic phase in the quantum Potts model where it has been suggested (like in the ROM model) that the transition becomes continuous at zero temperature [23]. These are subjects for future research.

## Acknowledgements

F.R. is grateful to the Foundation for Fundamental Research of Matter (FOM) in The Netherlands for financial support through contract number FOM-67596. The authors acknowledge hospitality at the ISI (Turin, Italy), where part of the work was done.

## Appendix A. Other discretizations of the coherent-state path integral

The coherent-state path integral has an obvious expression in the continuum limit  $M \rightarrow \infty$ ,  $d\tau \rightarrow 0$ . However, that is a dangerous limit, which may introduce problems that do not occur in its finite  $M$  expression [41]. A typical case is the following sum over Matsubara frequencies  $\omega = 2\pi nT$  ( $n = 1, \dots, M$ )

$$P = \sum_{\omega} \ln(\beta\mu - i\Omega_{\omega}) - \mathcal{N}, \quad (\text{A.1})$$

where  $\mathcal{N}$  is an appropriate normalization and

$$\Omega_{\omega} = iMT(1 - e^{i\omega}) \approx \omega, \quad (|\omega| \ll 1). \quad (\text{A.2})$$

This sum can be carried out after expanding in powers of  $e^{i\omega}$  and yields in the limit  $M \rightarrow \infty$

$$P = \ln[(1 + \varepsilon\mu)^M - 1] \rightarrow \ln[e^{\beta\mu} - 1], \quad (\text{A.3})$$

provided we choose  $\mathcal{N} = M \ln M$ . The common approach, however, is to approximate  $\Omega_{\omega} \approx \omega$ , choose  $\mathcal{N} = \sum_{\omega} \log(-i\omega)$ , and to extend to sum from  $-M/2 < n \leq M/2 \rightarrow -\infty < n < \infty$ , which yields the result

$$\tilde{P} = \ln 2 \sinh \frac{1}{2} \beta\mu = \ln[e^{\beta\mu} - 1] - \beta\mu/2. \quad (\text{A.4})$$

This ill-defined procedure thus brings a different result for the non-singular part. Those terms also show up in the zero point energy, that is to say, terms that may arise when normal-ordering of the creation and annihilation operators. The common approach also yields a different answer for the first derivative of  $P$  wrt  $\mu$ . For the second derivative the convergence is quick enough to yield the same answer in both approaches.

## Appendix B. Normalization of the path integral: free spherical spins in a field

The second term in Eq. (44) is

$$A_1 = \left( -m\sigma + \frac{m}{1 - a^M} + \frac{\Gamma^2}{\mu^2} \right) \sum_j \varepsilon\mu_j. \quad (\text{B.1})$$

As expected, it vanishes when  $\mu$  is taken at the saddle point. The quadratic fluctuations yield

$$\begin{aligned}
 -2A_2 = \varepsilon^2 \sum_j \mu_j^2 \left( \frac{m}{1-a^M} + \frac{\Gamma^2}{\mu^2} \right) \\
 + \varepsilon^2 \sum_{jj'} \mu_j \mu_{j'} \left( \frac{ma^M}{(1-a^M)^2} + \frac{\Gamma^2 a^{|j-j'|} + a^{M-|j-j'|}}{\mu^2 (1-a^M)} \right). \tag{B.2}
 \end{aligned}$$

The  $\mu_j^2$  and  $\mu_j \mu_{j'}$  terms can be calculated by going to Fourier space. Using the equation of motion  $A_2$  can be rewritten as

$$\begin{aligned}
 -2A_2 = M\varepsilon^2 \sum_{\omega} \mu_{\omega} \mu_{-\omega} \left[ \sigma + \delta_{\omega,0} \frac{Mme^{\beta\mu}}{(e^{\beta\mu} - 1)^2} \right] \\
 + \frac{\Gamma^2}{\mu^2} \left[ \left( \frac{1}{1-ae^{i\omega\varepsilon}} + \frac{ae^{-i\omega\varepsilon}}{1-ae^{-i\omega\varepsilon}} \right) \right]. \tag{B.3}
 \end{aligned}$$

Thus, the  $\mu$ -integrals yield

$$Z = \frac{C_M}{(2\pi MN\sigma)^{M/2}} \sqrt{\frac{\sigma + (2M\gamma/\beta\mu)}{\sigma + Mme^{\beta\mu}/(e^{\beta\mu} - 1)^2 + (2M\gamma/\beta\mu)}} e^{-A_0 - 1/2D}, \tag{B.4}$$

$$D = \sum_{\omega} \ln \frac{1 + a^2 + \gamma/\sigma(1 - a^2) - ae^{i\omega\varepsilon} - ae^{-i\omega\varepsilon}}{(1 - ae^{i\omega\varepsilon})(1 - ae^{-i\omega\varepsilon})}. \tag{B.5}$$

The  $\omega$ -sums can be carried out using

$$\sum_{\omega} \ln(1 - be^{\pm i\omega\varepsilon}) = \ln(1 - b^M). \tag{B.6}$$

For the leading behavior at  $\Gamma \neq 0$  we get with  $b = 1 - \Gamma\sqrt{2\varepsilon/\mu}$

$$D \approx M \ln \frac{1}{b} + 2 \ln(1 - b^M) \approx \sqrt{M} \sqrt{\frac{2\beta\Gamma^2}{\mu}}. \tag{B.7}$$

If we choose

$$C_M = (2\pi MN\sigma)^{M/2}, \tag{B.8}$$

it follows for  $\Gamma \neq 0$  that the free energy has, on top of the extensive part  $TA_0$ , a non-universal contribution of order  $N^0 M^{1/2}$ . For  $\Gamma$  strictly equal to 0, there is a universal term  $N^0 \ln M$ . Both terms are non-extensive and can be omitted if one first takes  $N$  large and then  $M$  [34]. Actually, this is also the limit that underlies the saddle point approximation. Physically it is also the natural limit, as for fixed small  $T$  the  $M = \infty$  limit is reached already for  $M \sim 1/T$  independent of  $N$ . This example shows that the extensive part of the free energy of quantum spherical spins is a well defined, natural object. Non-extensive parts are more delicate.

### Appendix C. Critical endpoint in the static approximation: Ising case

Here we give the equations which yields the critical endpoint in the SA in the Ising case (see also [31] for the original derivation).

Starting from Eq. (107) we define the function  $g(x)$ ,

$$g(q) = q - \overline{\Phi(x)^{-1} x^2 \sinh \Phi(x)}, \quad (\text{C.1})$$

where  $\Phi(x) = \sqrt{\beta^2 \Gamma^2 + \beta^2 \lambda x^2}$  and  $\lambda = pq^{p-1}/2$  and the average  $\overline{(\cdot)}$  is defined by

$$\overline{A(x)} = \frac{\int_{-\infty}^{\infty} dp_x A(x)}{\int_{-\infty}^{\infty} dp_x \cosh(x)}. \quad (\text{C.2})$$

The paramagnetic phases are found by solving the equation  $g(q_d) = 0$ . This yields one solution at very high temperatures and three solutions at lower temperatures. Of these three solutions two of them are stable (the ones with largest and smallest values of  $q_d$ ) while the other one (that with an intermediate value of  $q_d$ ) is unstable. This is the same scenario as in the spherical model. The critical point is then determined by the coalescence of these two stable solutions. This gives the equations

$$g(q_d) = \left( \frac{\partial g}{\partial q} \right)_{q=q_d} = \left( \frac{\partial^2 g}{\partial q^2} \right)_{q=q_d} = 0. \quad (\text{C.3})$$

These three equations read

$$q_d = f_c^{(1)}(q_d) = q_d, \quad (\text{C.4})$$

$$\frac{\beta^2 p(p-1)}{4} q_d^{p-2} f_c^{(2)}(q_d) = 1, \quad (\text{C.5})$$

$$(2-p) f_c^{(2)}(q_d) = \frac{\beta^2 p(p-1) q_d^{p-1}}{4} f_c^{(3)}(q_d), \quad (\text{C.6})$$

where  $f_c^{(1)}, f_c^{(2)}, f_c^{(3)}$  are the first three cumulants associated to the functions  $f^{(n)}$  ( $n = 1, 2, 3$ )

$$f^{(1)} = \overline{\Phi^{-1} x^2 \sinh \Phi}, \quad (\text{C.7})$$

$$f^{(2)} = \overline{\Phi^{-3} x^4 (\Phi \cosh \Phi - \sinh \Phi)}, \quad (\text{C.8})$$

$$f^{(3)} = \overline{\Phi^{-5} x^6 (\Phi^2 \sinh \Phi - 3\Phi \cosh \Phi + 3 \sinh \Phi)}. \quad (\text{C.9})$$

These equations can be exactly solved yielding  $T_{cp}, \Gamma_{cp}, q_d^{cp}$  for different values of  $p$ . Is not difficult to generalize this set of equations beyond the SA in the general case.

### Appendix D. Equations for the energy in the Ising case

In this appendix we give the exact expressions for the internal energy used to compute the latent heat in Section 4.2. We start from Eq. (91) by evaluating the derivative

$u = \partial\beta f / \partial\beta$ . This yields

$$u = -\frac{\partial C}{\partial\beta} - \frac{\beta(m-1)q^p}{2} - \frac{\beta}{2M^2} \sum_{u'} (q_d(t-t'))^p + \beta(m-1)q\lambda + \frac{\beta}{M^2} \sum_{u'} q_d(t-t')\lambda(t-t') - \frac{1}{m} \frac{\int_{-\infty}^{\infty} dp_x \Xi^{m-1}(x) \partial\Xi / \partial\beta}{\int_{-\infty}^{\infty} dp_x \Xi^m(x)}, \quad (D.1)$$

where  $C$  and  $\Xi(x)$  were defined in Eqs. (84) and (94) respectively and  $dp_x$  is the Gaussian measure. Doing the last integral by parts and rearranging terms we get the final expression

$$u = -\Gamma \coth\left(\frac{2\beta\Gamma}{M}\right) - \frac{\beta(m-1)q^p}{2} - \frac{\beta}{2M^2} \sum_{u'} (q_d(t-t'))^p + \frac{\Gamma}{\sinh(2\beta\Gamma/M)} q_d(1). \quad (D.2)$$

In the continuum limit  $M \rightarrow \infty$  the  $q_d(t)$  becomes a continuous function of time yielding

$$u = \left(\frac{\partial q_d}{\partial t}\right)_{t=0} - \frac{\beta(m-1)q^p}{2} - \frac{1}{2} \int_0^\beta (q_d(t))^p dt. \quad (D.3)$$

In the  $QP^<$  phase at zero temperature in the large  $\Gamma$  regime we have  $q_d(t) \sim \exp(-t\Gamma)$  yielding  $u \sim -\Gamma - 1/(2p\Gamma)$ . Note that the SA is only exact in the limit  $p \rightarrow \infty$  where the energy is given by  $u = -\Gamma$ .

It is also easy to check that in the SA the energy is simply given by

$$u = -\frac{\beta}{2} (q_d^p - (1-m)q^p) - \beta\Gamma^2 \langle\langle \overline{\sinh(T(x,z))/T(x,z)} \rangle\rangle, \quad (D.4)$$

where the averages  $\overline{(\cdot)}$ ,  $\langle\langle(\cdot)\rangle\rangle$  and  $T(x,z)$  were previously defined in Eqs. (99), (106) and (103), respectively.

## References

- [1] S. Sachdev, in: Hao Bailin (Ed.), *Statphys*, vol. 19, World Scientific, Singapore 1996.
- [2] H. Rieger, A.P. Young, in: M. Rubí, C. Pérez-Vicente (Eds.), *Complex Behavior of Glassy Systems*, Lecture Notes in Physics, Springer, Berlin, 1997, p. 256.
- [3] S.L. Sondhi, S.M. Girvin, J.P. Carini, D. Shahar, *Rev. Mod. Phys.* 69 (1997) 315.
- [4] B.K. Chakrabarty, A. Dutta, P. Sen, *Quantum Ising Phases and Transitions in Transverse Ising models*, Lecture Notes in Physics, vol. M41, Springer, Berlin, 1996.
- [5] S. Sachdev, A.P. Young, *Phys. Rev. Lett.* 78 (1997) 2220.
- [6] J.P. Bouchaud, M. Mezard, *J. Physique I (Paris)* 4 (1994) 1109.
- [7] E. Marinari, G. Parisi, F. Ritort, *J. Phys. A (Math. Gen.)* 27 (1994) 7615.

- [8] E. Marinari, G. Parisi, F. Ritort, *J. Phys. A (Math. Gen.)* 27 (1994) 7647.
- [9] K. Binder, A.P. Young, *Rev. Mod. Phys.* 58 (1986) 801.
- [10] M. Mézard, G. Parisi, M.A. Virasoro, *Spin Glass Theory and Beyond*, World Scientific, Singapore 1987.
- [11] K.H. Fischer, J.A. Herz, *Spin Glasses*, Cambridge University Press, Cambridge 1991.
- [12] T.R. Kirkpatrick, D. Thirumalai, *Phys. Rev. B* 36 (1987) 5388.
- [13] T.R. Kirkpatrick, P.G. Wolynes, *Phys. Rev. B* 36 (1987) 8552.
- [14] Th.M. Nieuwenhuizen, Complexity as the driving force for glassy transitions, in: M. Rubí, C. Pérez-Vicente (Eds.), *Complex Behavior of Glassy Systems*, Lecture Notes in Physics, Springer, Berlin, 1997, p. 139.
- [15] J.H. Gibbs, E.A. Di Marzio, *J. Chem. Phys.* 28 (1958) 373.
- [16] G. Adams, J.H. Gibbs, *J. Chem. Phys.* 43 (1965) 139.
- [17] D. Alvarez, S. Franz, F. Ritort, *Phys. Rev. B* 54 (1996) 9756.
- [18] Th.M. Nieuwenhuizen, 1996, preprint.
- [19] Th. M. Nieuwenhuizen, *Phys. Rev. Lett.* 79 (1997) 1317.
- [20] F. Ritort, *Phys. Rev. B* 55 (1997) 14096.
- [21] See also F. Ritort, Classical and quantum behavior in mean-field glassy systems, in: M. Rubí, C. Pérez-Vicente (Eds.), *Complex Behavior of Glassy Systems*, Lecture Notes in Physics, Springer, Berlin, 1997, p. 122.
- [22] A.J. Bray, M.A. Moore, *J. Phys. C* 13 (1980) L655.
- [23] T. Senhil, S.N. Majumdar, *Phys. Rev. Lett.* 76 (1996) 3001.
- [24] A. Crisanti, H.J. Sommers, *Z. Phys. B* 92 (1992) 341.
- [25] A. Crisanti, H. Horner, H.-J. Sommers, *Z. Phys. B* 92 (1993) 257.
- [26] D.J. Gross, M. Mezard, *Nucl. Phys. B* 240 (1984) 431.
- [27] E. Gardner, *Nucl. Phys. B* 257 (1985) 747.
- [28] Y.Y. Goldschmidt, *Phys. Rev. B* 41 (1990) 4858.
- [29] B. Derrida, *Phys. Rev. B* 24 (1981) 2613.
- [30] P. Mottishaw, *Europhys. Lett.* 1 (1986) 409.
- [31] V. Dobrosavljevic, D. Thirumalai, *J. Phys. A* 22 (1990) L767.
- [32] L. De Cesare, K. Lubierska-Walasek, I. Rabuffo, K. Walasek, *J. Phys. A* 29 (1996) 1605.
- [33] S. Franz, G. Parisi, Phase diagram of glassy systems in an external field, preprint cond-mat/9701033.
- [34] Th.M. Nieuwenhuizen, *Phys. Rev. Lett.* 74 (1995) 4293.
- [35] In the case  $p=3$ ,  $m\sigma=1$ ,  $m=2$  one has  $(T_{cep}, \Gamma_{cep})=(0.4070, 0.89001)J$ ;  $(T_{mcp}, \Gamma_{mcp})=(0.37506, 0.95379)J$ .
- [36] R. Pandit, M. Schick, M. Wortis, *Phys. Rev. B* 26 (1982) 5112.
- [37] G. Forgacs, R. Lipowsky, Th.M. Nieuwenhuizen, in: C. Domb, J.L. Lebowitz (Eds.), *Phase Transitions and Critical Phenomena* vol. 14, Academic, New York, 1991, pp. 135.
- [38] J.E. Rutledge, P. Taborek, *Phys. Rev. Lett.* 69 (1992) 937.
- [39] D. Bonn, H. Kellay, G.H. Wegdam, *J. Phys.: Condens. Matter* 6 (1994) A389.
- [40] H. Kellay, D. Bonn, J.M. Meunier, *Phys. Rev. Lett.* 71 (1994) 2607.
- [41] J.W. Negele, H. Orland, *Quantum Many-Particle Systems*, Addison-Wesley, Redwood City, 1988.
- [42] J.W. Hartman, P.B. Weichman, *Phys. Rev. Lett.* 74 (1995) 4584.
- [43] T. Voita, *Phys. Rev. B* 53 (1996) 710.
- [44] T. Voita and M. Schreiber, *Phys. Rev. B* 53 (1996) 8211.
- [45] J.M. Kosterlitz, D.J. Thouless, R.C. Jones, *Phys. Rev. Lett.* 36 (1976) 1217.
- [46] Th.M. Nieuwenhuizen, *Phys. Rev. B* 31 (1985) R7487.
- [47] Th.M. Nieuwenhuizen, *Phys. Rev. Lett.* 74 (1995) 4289.
- [48] Regularisation terms correspond to  $M$  dependent expressions which yield the same  $M \rightarrow \infty$  limit.
- [49] J. Miller, D. Huse, *Phys. Rev. Lett.* 70 (1993) 3147.
- [50] J. Ye, S. Sachdev, N. Read, *Phys. Rev. Lett.* 70 (1993) 4011.
- [51] N. Read, S. Sachdev, *Phys. Rev. B* 52 384.
- [52] G. Büttner, K.D. Usadel, *Phys. Rev. B* 41 (1990) 428.
- [53] Y.Y. Goldschmidt, P.Y. Lai, *Phys. Rev. Lett.* 64 (1990) 2467.
- [54] H. Ishii, Y. Yamamoto, *J. Phys. C* 18 (1985) 6225.
- [55] H. Ishii, Y. Yamamoto, *J. Phys. C* 20 (1987) 6053.
- [56] D. Lancaster, F. Ritort, *J. Phys. A* 30 (1997) L41.
- [57] For a recent investigation see also, P. Sen, P. Ray, B.K. Chakrabarti, preprint cond-mat/9705297.

- [58] For a numerical study in two and three dimensions see, M. Guo, R.N. Bhatt, D.A. Huse, *Phys. Rev. Lett.* 72 (1994) 4137.
- [59] H. Rieger, A.P. Young, *Phys. Rev. Lett.* 72 (1994) 4141.
- [60] J.V. Alvarez, F. Ritort, *J. Phys. A* 29 (1996) 7355.
- [61] Note that the static ansatz, in the general case, cannot be in agreement with Eq. (97) where the one dimensional structure of the Hamiltonian  $\Theta(x, \{\sigma_t\})$  prevents the  $q_d(t - t')$  to be time independent.
- [62] We suppose that the size of the system is infinite from the beginning or that the typical time scale involved in the adiabatic process grows with the size of the system much slower than any exponentially long time scale. Obviously, for weak first order phase transitions this assertion is no longer true.